Constructing exact representations of quantum many-body systems with deep neural networks

Giuseppe Carleo

Center for Computational Quantum Physics, Flatiron Institute,
162 5th Avenue, New York, NY 10010, USA and
Institute for Theoretical Physics, ETH Zurich, Wolfgang-Pauli-Str. 27, 8093 Zurich, Switzerland

Yusuke Nomura and Masatoshi Imada

Department of Applied Physics, The University of Tokyo,
7-3-1 Hongo, Bunkyo-ku, Tokyo 113-8656, Japan

We develop a constructive approach to generate artificial neural networks representing the exact ground states of a large class of many-body lattice Hamiltonians. It is based on the deep Boltzmann machine architecture, in which two layers of hidden neurons mediate quantum correlations among physical degrees of freedom in the visible layer. The approach reproduces the exact imaginary-time Hamiltonian evolution, and is completely deterministic. In turn, compact and exact network representations for the ground states are obtained without stochastic optimization of the network parameters. The number of neurons grows linearly with the system size and total imaginary time, respectively. Physical quantities can be measured by sampling configurations of both physical and neuron degrees of freedom. We provide specific examples for the transverse-field Ising and Heisenberg models by implementing efficient sampling. As a compact, classical representation for many-body quantum systems, our approach is an alternative to the standard path integral, and it is potentially useful also to systematically improve on numerical approaches based on the restricted Boltzmann machine architecture.

INTRODUCTION

A tremendous amount of successful developments in quantum physics builds upon the mapping between many-body quantum systems and effective classical theories. The probably most well known mapping is due to Feynman, who introduced an exact representation of many-body quantum systems in terms of statistical summations over classical particles trajectories [1]. Effective classical representations of quantum many-body systems are however not unique, and other approaches rely on different inspiring principles, such as perturbative expansions [2], or decomposition of interactions with auxiliary degrees of freedom [3, 4]. The classical representations of quantum states allow both for novel conceptual developments and efficient numerical simulations. On one hand, perturbative approaches based on the graphical resummation of classes of diagrams are at the heart of many-body analytical approaches in various fields of research, ranging from particle to condensed-matter physics [5]. On the other hand, several non-perturbative numerical methods for many-body quantum systems are also based on these mappings. Quantum Monte Carlo (QMC) methods are among the most successful numerical techniques, relying on continuos-space polymer representations [6–9], world-line lattice path integrals [10, 11], continuous time algorithm [12], summation of perturbative diagrams [13, 14]. Effective classical representations are also the building block of variational methods based on correlated many-body wave-functions [15]. Several successful variational techniques make extensive use of parametric representations of quantum states, where the effective parameters are determined by means of the variational principle [16–19]. In matrix-product and tensor-network-states the ground-state is expressed as a classical network [20, 21]. In general, finding alternative, efficient classical representations of quantum states can help establishing novel numerical and analytical techniques to study challenging open issues.

Recently, an efficient variational representation of many-body systems in terms of artificial neural networks, which consists of classical degrees of freedom, has been introduced [22]. Numerical results have shown that artificial neural networks can represent many-body states with high accuracy [22–31]. The majority of the variational approaches adopted so-far are based on shallow neural networks, called Restricted Boltzmann Machines (RBM), in which the physical degrees of freedom interact with an ensemble of hidden degrees of freedom (neurons). While shallow RBM states have promising features in terms of entanglement capacity [25, 32–34], only deep networks are guaranteed to provide a complete and efficient description of the most general quantum states [35, 36].

In this Paper we introduce a constructive approach to explicitly generate deep network structures corresponding to exact quantum many-body ground states. We demonstrate this construction for interacting lattice spin models, including the transverse-field Ising and Heisenberg models. Our constructions are fully deterministic, in stark contrast to the shallow RBM case, in which the numerical optimization of the network parameters is inevitable. The number of neurons required in the con-
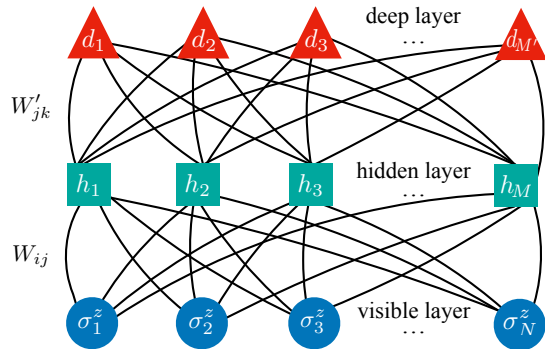
Figure 1. **Structure of deep Boltzmann machine**. Dots, squares, and triangles represent physical degrees of freedom (σ_i^z), hidden units (h_j), deep units (d_k), respectively. Solid curves represent interlayer couplings (W_{ij} and W'_{jk}).

struction scales only polynomially with the system size, thus the present approach constitutes a new family of efficient quantum-to-classical mappings exhibiting a prominent representational flexibility. Given as a simple set of iterative rules, these constructions can be used both as a self-standing tool, or to systematically improve results obtained with variational shallow networks. The latter improves the efficiency of the method because the numerically optimized shallow RBM states are already good approximations for ground states. Finally, we discuss sampling strategies from the generated deep networks and show numerical results for one-dimensional spin models.

CONSTRUCTION OF DEEP NEURAL STATES

The ground state of a generic Hamiltonian, $\mathcal{H}$, can be found through imaginary-time evolution, $|\Psi(\tau)\rangle = e^{-\tau\mathcal{H}}|\Psi_0\rangle$, for a sufficiently large $\tau \gg \Delta E^{-1}$. Here ΔE is the energy gap between the ground and the first excited state, and $|\Psi_0\rangle$ is an arbitrary initial state nonorthogonal to the exact ground state. For a finite system, the energy gap is typically finite, and the total propagation time needed to reach the ground state within an arbitrary given accuracy is expected to grow at most polynomially with the system size (for systems becoming gapless in the thermodynamic limit).

Here, we introduce a representation of the wave-function coefficients in terms of a deep Boltzmann machine (DBM) [37]. For the sake of concreteness, let us consider the case of N spins, described by the quantum numbers $|\sigma^z\rangle = |\sigma_1^z \ldots \sigma_N^z\rangle$. Then, we represent generic many-body amplitudes $\langle \sigma_1^z \ldots \sigma_N^z|\Psi\rangle \equiv \Psi(\sigma^z)$ in

the two-layer DBM form:

$$\Psi_{\mathcal{W}}(\sigma^z) = \sum_{\{h,d\}} \exp\left[\sum_i a_i\sigma_i^z + \sum_{ij}\sigma_i^z W_{ij}h_j + \right.$$
$$\left. + \sum_j b_j h_j + \sum_{jk} h_j d_k W'_{jk} + \sum_k b'_k d_k\right] \quad (1)$$

where we have introduced M hidden units h, M' deep units d, and a set of couplings and bias terms $\mathcal{W} \equiv (a,b,b',W,W')$. A sketch of the DBM architecture is shown in Fig. 1.

In the following, we specialize to the case of spin $1/2$, thus all the units are taken to be $\sigma^z, h, d = \pm 1$. This representation is the natural deep-network generalization of the shallow RBM, introduced as variational ansatz in Ref. [22]. As for the RBM form, also in this case direct connections between variables in the same layer are not allowed. A crucial difference is however that the layer of deep variables makes, in general, the evaluation of the wave-function amplitudes not possible analytically. At variance with RBM, the DBM form is known to be universal, as proven by Gao and Duan recently [35]. In order to find explicit expressions for the parameters $\mathcal{W}$ that represent $|\Psi(\tau)\rangle$ for arbitrary imaginary time, we start considering a second-order Trotter-Suzuki decomposition [10, 38]:

$$|\Psi(\tau)\rangle = \mathcal{G}_1(\delta_\tau/2)\mathcal{G}_2(\delta_\tau)\ldots\mathcal{G}_1(\delta_\tau)\mathcal{G}_2(\delta_\tau)\mathcal{G}_1(\delta_\tau/2)|\Psi_0\rangle, \quad (2)$$

where we have decomposed the Hamiltonian into two non-commuting parts, $\mathcal{H} = \mathcal{H}_1 + \mathcal{H}_2$, and introduced the short-time propagators $\mathcal{G}_\nu(\delta_\tau) = e^{-\mathcal{H}_\nu\delta_\tau}$. The problem of finding an exact representation for $|\Psi(\tau)\rangle$ then reduces to finding an exact representation for each of the two type of propagators. As shown in the following concrete examples for paradigmatic spin models, thanks to the high representability of DBM, the imaginary time evolution can be tracked exactly by dynamically modifying the DBM network structure. In practice, this is achieved either by changing parameters $\mathcal{W}$ at each step of the imaginary time evolution, or by introducing additional parameters in $\mathcal{W}$, adding new neurons and creating new connections in the network.

Transverse-Field Ising model

We start considering the transverse-field Ising (TFI) model on an arbitrary interaction graph. In this case, we decompose the Hamiltonian into two parts: $\mathcal{H}_1 = -\sum_l \Gamma_l \sigma_l^x$, and $\mathcal{H}_2 = \sum_{l<m} V_{lm}\sigma_l^z\sigma_m^z$, where σ denote Pauli matrices, $\Gamma_l \,(>0)$ are site-dependent transverse fields, and V_{lm} are arbitrary coupling constants.
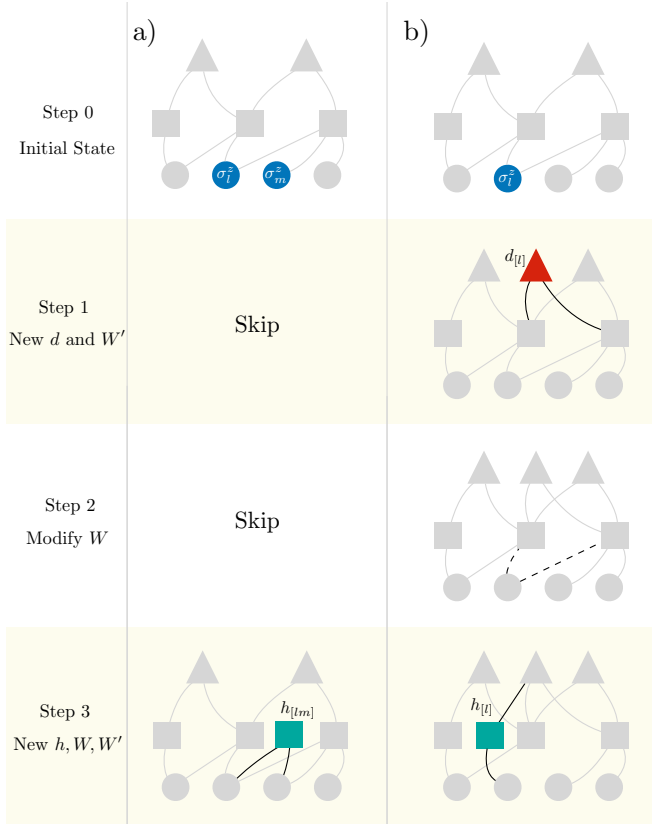
Figure 2. **Construction of exact DBM representations of transverse-field Ising model**. In this example, a step of imaginary-time evolution is shown, for the case of the 1-dimensional transverse-field Ising model. Dots represent physical degrees of freedom (σ_i^z), squares represent hidden units (h_j), triangles represent deep units (d_k). In each panel, upper networks are the initial state with arbitrary network form, and the bottom networks are the final states, after application of the propagator. Intermediate steps illustrate how the network is modified, where the relevant modified couplings at each step are highlighted in black. The highlighted solid and dashed curves indicate new and vanishing couplings, respectively. (a) Shows the diagonal (interaction) propagator being applied to the highlighted blue spins. This introduces a hidden unit (green) connected only to the two physical spins. In (b) the off-diagonal (transverse-field) propagator is applied, acting on the blue physical spin. Here, we then add one deep unit (red triangle), and a hidden unit (green) mediating visible-deep interactions.

In order to implement the mapping to a DBM, we first consider the action of the diagonal propagator $e^{-\delta_\tau V_{lm}\sigma_l^z\sigma_m^z}$, acting on a bond V_{lm}. In this case, the goal of finding an exact DBM representation can be rephrased as finding solutions to

$$\langle\sigma^z|e^{-\delta_\tau V_{lm}\sigma_l^z\sigma_m^z}|\Psi_{\mathcal{W}}\rangle = C\Psi_{\bar{\mathcal{W}}}(\sigma^z), \qquad (3)$$

i.e. finding a set of new parameters $\bar{\mathcal{W}}$ that exactly reproduces the imaginary time evolution on the left hand side. Here C is an arbitrary finite normalization constant. The diagonal propagator introduces an interaction between

two visible, physical spins, which is not directly available in the DBM architecture. This interaction can be mediated by a new hidden unit in the first layer, $h_{[lm]}$ which is only connected to the visible spins on that bond, i.e. $\bar{W}_{l[lm]}$ and $\bar{W}_{m[lm]}$ are finite, but $\bar{W}_{i[lm]} = 0, \forall i \neq l, m$ and $\bar{W}'_{j[lm]} = 0, \forall j$ [see Fig. 2(a)].

More concretely, the new wave function has then the form:

$$\Psi_{\bar{\mathcal{W}}}(\sigma^z) = \sum_{h_{[lm]}} e^{\sigma_l^z W_{l[lm]}h_{[lm]}+\sigma_m^z W_{m[lm]}h_{[lm]}}\Psi_{\mathcal{W}}(\sigma^z)$$

$$= 2\cosh\left(\sigma_l^z W_{l[lm]} + \sigma_m^z W_{m[lm]}\right)\Psi_{\mathcal{W}}(\sigma^z). \,(4)$$

Equation (79) is then satisfied if

$$e^{-\delta_\tau V_{lm}\sigma_l^z\sigma_m^z} = 2C\cosh\left(\sigma_l^z W_{l[lm]} + \sigma_m^z W_{m[lm]}\right) \quad (5)$$

for all the possible values of σ_l^z and σ_m^z. By means of a useful identity [Eq. (16) in Methods], the new parameters $W_{l[lm]}$ and $W_{m[lm]}$ are given by

$$W_{l[lm]} = \frac{1}{2}\text{arcosh}\left(e^{2|V_{lm}|\delta_\tau}\right) \qquad (6)$$

$$W_{m[lm]} = -\text{sgn}(V_{lm}) \times W_{l[lm]}. \qquad (7)$$

In this way the classical two-body interaction can, in general, be represented exactly by the shallow RBM.

Next, to exactly represent the off-diagonal propagator $e^{\delta_\tau \Gamma_l \sigma_l^x}|\Psi_{\mathcal{W}}\rangle$, we must solve:

$$\cosh(\Gamma_l\delta_\tau)\Psi_{\mathcal{W}}(\sigma^z) + \sinh(\Gamma_l\delta_\tau)\Psi_{\mathcal{W}}(\sigma_l^z \to -\sigma_l^z) =$$
$$= C\Psi_{\bar{\mathcal{W}}}(\sigma^z) \quad (8)$$

for the new weights $\bar{\mathcal{W}}$, and for an appropriate finite normalization constant C. In this case, one possible solution is obtained by adding one deep $d_{[l]}$ and one hidden $h_{[l]}$ neurons. For $d_{[l]}$, we create new couplings $W'_{j[l]}$ to the existing hidden neurons h_j which are connected to σ_l^z. We simultaneously allow for changes in the existing parameters. By the procedure given in Methods, after applying the off-diagonal propagator for the site l, a solution of Eq.(8) is found by the matching condition of the hidden unit interactions on the left and the right hand sides of Eq.(8). Overall, the solution results in a three-step process [Fig. 2(b)]: First, the hidden units attached to σ_l^z are connected to the newly introduced deep unit $d_{[l]}$ as

$$W'_{j[l]} = -W_{lj} \qquad (9)$$

(see Eq.(30)). Second, all the hidden units previously connected to the spin σ_l^z lose their connection, i.e., $\bar{W}_{lj} = 0, \forall j$. Third, the spin σ_l^z and the deep unit $d_{[l]}$ are connected to the new hidden unit, $h_{[l]}$, through the interaction $W_{l[l]}$ and $W'_{[l][l]}$, respectively as

$$W_{l[l]} = \frac{1}{2}\text{arcosh}\left(\frac{1}{\tanh(\Gamma_l\delta_\tau)}\right), \qquad (10)$$

$$W'_{[l][l]} = -W_{l[l]}. \qquad (11)$$

Using the given expressions for the parameters $\bar{\mathcal{W}}$ we can then exactly implement a single step of imaginary-time evolution. The full imaginary-time evolution is achieved by applying the above procedure for $\mathcal{H}_1$ and $\mathcal{H}_2$ alternately and repeatedly. Example applications of these rules, for both the diagonal and the off-diagonal propagators are shown in Fig. 2.

Heisenberg model

We now consider the anti-ferromagnetic Heisenberg (AFH) model, on bipartite lattices. In one dimension, we decompose the Hamiltonian into odd and even bonds: $\mathcal{H}_1 = \sum_{\langle l,m \rangle}^{\text{odd}} \mathcal{H}_{lm}^{\text{bond}}$ and $\mathcal{H}_2 = \sum_{\langle l,m \rangle}^{\text{even}} \mathcal{H}_{lm}^{\text{bond}}$, with $\mathcal{H}_{lm}^{\text{bond}} = J\left(\sigma_l^x \sigma_m^x + \sigma_l^y \sigma_m^y + \sigma_l^z \sigma_m^z\right)$, where σ denote Pauli matrices. Because the bond Hamiltonian $\mathcal{H}_{lm}^{\text{bond}}$ is a building block also in higher dimensional models, construction of an exact DBM representation of the ground states can be achieved by finding solutions for the bond-propagator $\langle \sigma^z | e^{-\delta_\tau \mathcal{H}_{lm}^{\text{bond}}} | \Psi_{\mathcal{W}} \rangle = C \langle \sigma^z | \Psi_{\bar{\mathcal{W}}} \rangle$, where the parameters $\bar{\mathcal{W}}$ are such that the previous equation is satisfied for all the possible $\langle \sigma^z |$, and for an arbitrary finite normalization constant C. More explicitly, we need to satisfy

$$
\begin{aligned}
&\delta_{\sigma_l^z, \sigma_m^z} e^{-J\delta_\tau} \Psi_{\mathcal{W}}(\sigma^z) + (1 - \delta_{\sigma_l^z, \sigma_m^z}) e^{J\delta_\tau} \cosh(2J\delta_\tau) \times \\
&(\Psi_{\mathcal{W}}(\sigma^z) - \tanh(2J\delta_\tau)\Psi_{\mathcal{W}}(\sigma_l^z \leftrightarrow \sigma_m^z)) = C\Psi_{\bar{\mathcal{W}}}(\sigma^z).
\end{aligned}
\tag{12}
$$

The basic strategy of finding a solution for Eq.(12) is similar to that for Eq.(8) in the transverse Ising model. Several possibilities arise when looking for solutions of the bond-propagator equation, Eq. (12). The existence of non-equivalent solutions prominently shows the non-uniqueness of DBM structure to represent the very same state and, at the same time, provides us flexibility in designing DBM architectures. Here, we show three concrete constructions. See Methods and Supplementary Information (II-B) for a detailed derivation of the DBM construction for the Heisenberg model, including anisotropic and bond-disordered coupling cases.

1 deep, 3 hidden

The first construction is dubbed "*1 deep, 3 hidden*" (1d-3h). It amounts to adding an extra deep neuron, $d_{[lm]}$, and three more hidden neurons to satisfy Eq. (12). A crucial difference with respect to the TFI model is that the introduced deep spin $d_{[lm]}$ has a constraint depending on the state of the spins on the bond: σ_l^z and σ_m^z. Specifically, when $\sigma_l^z = \sigma_m^z$ the deep spin is constrained to be $d_{[lm]} = \sigma_l^z = \sigma_m^z$, whereas when $\sigma_l^z \neq \sigma_m^z$, its value is unconstrained. From a pictorial point of view, the action of the bond propagator is a four-step process [see

Fig. 3(a)]. Starting from a given initial network (uppermost structures in Fig. 3), $d_{[lm]}$ is added and connected, through $W'_{j[lm]}$ given in Eq. (38), to the existing hidden units h_j connected to σ_l^z and σ_m^z. Second, spin σ_l^z is disconnected to all hidden units and reconnected to those hidden units the spin σ_m^z is attached to [see Eq. (37)]. Third, two new hidden units are introduced. One of the hidden units, $h_{[lm1]}$, mediates the interaction between σ_l^z and $d_{[lm]}$ [Eq. (41)], and the other hidden unit $h_{[lm2]}$ mediates a direct spin-spin interaction between σ_l^z and σ_m^z [Eq. (42)]. Fourth, a further hidden unit connected to σ_l^z, σ_m^z and $d_{[lm]}$ is inserted, in such a way that the constraint previously described is satisfied. For all but the last step, the DBM weights are real-valued. In the last step instead the constraint is enforced by introducing imaginary-valued interactions (dotted lines in Fig. 3), referred to the "$i\pi/6$" trick, resulting in a sign-problem free global term $\cos(\pi/6(\sigma_l^z + \sigma_m^z - d_{[lm]}))$ after the summation over ± 1 for the lastly added hidden unit $h_{[lm3]}$: $\sum_{h_{[lm3]}=\pm 1} \exp[i\pi/6(\sigma_l^z + \sigma_m^z - d_{[lm]})h_{[lm3]}]$. The constraint mentioned above is assured by this cosine term.

2 deep, 6 hidden

The second construction is dubbed "*2 deep, 6 hidden*" (2d-6h), and is more similar to the lattice path-integral formulation. In this representation, we introduce two auxiliary deep spins per bond, $d_{[l]}$ and $d_{[m]}$ with constraint $d_{[l]} + d_{[m]} = \sigma_l^z + \sigma_m^z$, and six hidden neurons. The action of the bond propagator is schematically illustrated in Fig. 3(b): first, two deep units $d_{[l]}$ and $d_{[m]}$ are introduced, connecting, respectively, to the hidden units spins σ_l^z and σ_m^z are attached to [see Eqs. (44), (45)]. Second, all the connections between spins σ_l^z, σ_m^z and hidden units h_j are cut off [Eqs. (46), (47)]. Third, four hidden units $h_{[lm1]}, \ldots, h_{[lm4]}$ are introduced, to mediate interactions between the two deep units and the physical spins l, m [Eqs. (50), (51)]. Finally, two hidden units $h_{[lm5]}$ and $h_{[lm6]}$ are introduced, connecting both to $d_{[l]}, d_{[m]}$ and σ_l^z, σ_m^z with imaginary-valued weights. The last step realizes the constraint $d_{[l]} + d_{[m]} = \sigma_l^z + \sigma_m^z$, through the "$i\pi/4$, $i\pi/8$" trick discussed in Methods and Supplementary Information (II-B.2).

In this representation, if the hidden neurons are traced out, the imaginary-time evolution becomes equivalent to that of the path-integral Monte Carlo method. More specifically, the number of deep neurons introduced at each time slice is exactly the same as the number of visible spins, and the deep neurons at each time slice can be regarded as additional classical spin degrees of freedom in the path-integral. Moreover, the constraint $d_{[l]} + d_{[m]} = \sigma_l^z + \sigma_m^z$ ensures that the total magnetization is conserved at each time slice. Finally, the W and W' interactions reproduce the matrix element of $\exp(-\delta_\tau \mathcal{H}_{lm}^{\text{bond}})$ between neighboring time slices. See
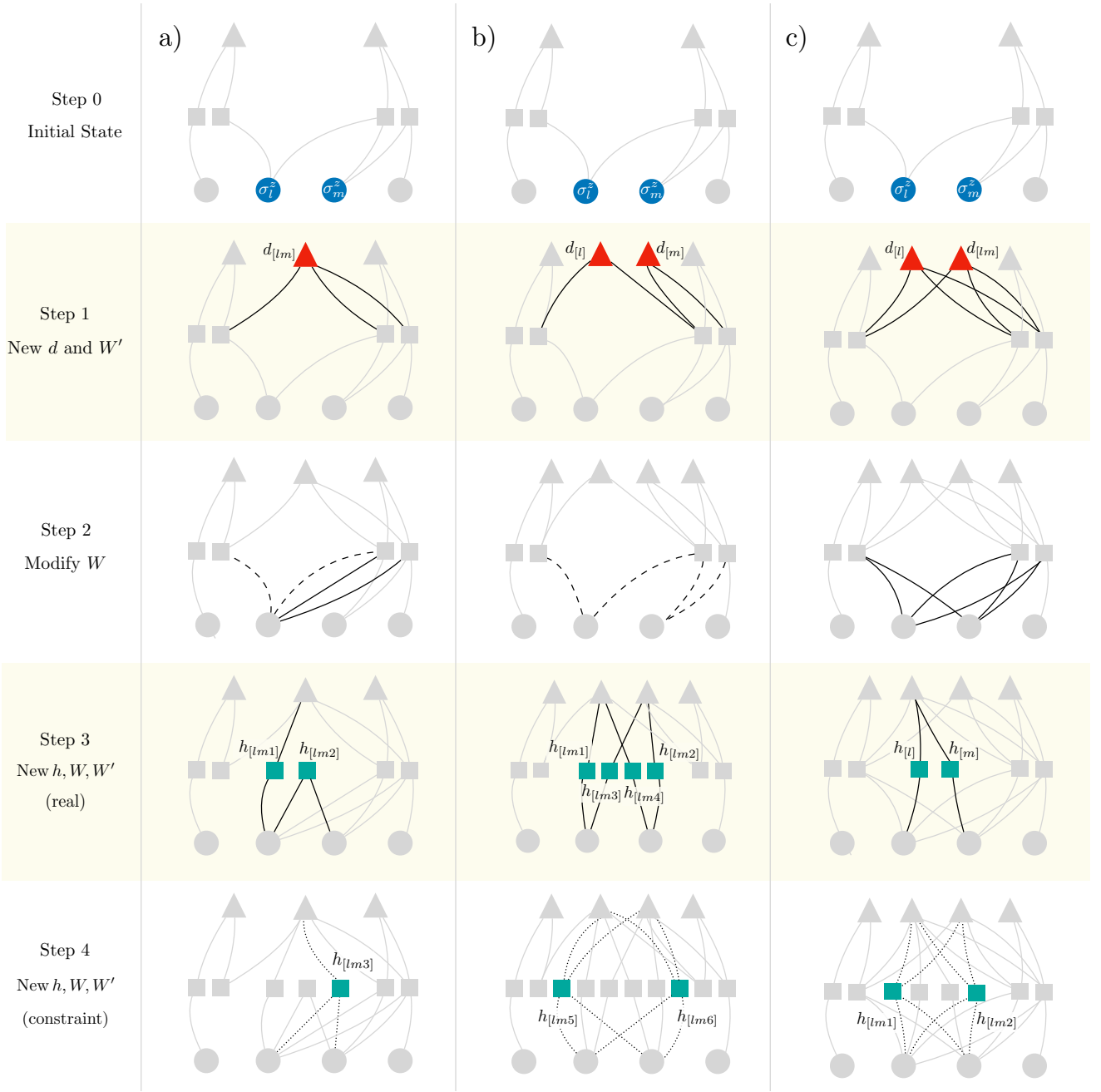
Figure 3. **Construction of exact DBM representations of Heisenberg models**. In this example, a time step of imaginary-time evolution is shown, for the case of the 1-dimensional antiferromagnetic Heisenberg model. Dots represent physical degrees of freedom (σ_i^z), squares represent hidden units (h_j), triangles represent deep units (d_k). The three panels (a,b,c) represent different possible explicit constructions. In each panel, upper networks are the initial state with arbitrary network form, and the bottom networks are the final states, after application of the propagator. Intermediate steps illustrate how the network is modified, where the relevant modified weights at each step are highlighted in black. In those diagrams, dashed lines indicate that the corresponding weights are set to zero, and dotted lines indicate complex-valued weights. The three panels correspond to the (a) *1 deep, 3 hidden* (1d-3h), (b) *2 deep, 6 hidden* (2d-6h), and (c) *2 deep, 4 hidden* (2d-4h) constructions (see text for a more detailed explanation of the individual steps characteristic of each construction).

Supplementary Information (II-B.2) for more detail on this point.

2 deep, 4 hidden

A further possible solution to Eq. (12) is dubbed "*2 deep, 4 hidden*" (2d-4h) construction. In this case, we

introduce two auxiliary deep variables $d_{[l]}$ and $d_{[lm]}$. We also introduce four hidden units $h_{[l]}$, $h_{[m]}$, $h_{[lm1]}$, and $h_{[lm2]}$. Before the imaginary time evolution, $e^{-\delta_\tau \mathcal{H}_{lm}^{\text{bond}}}$, the physical variables σ_n^z ($n = l$ or m) are already coupled to each hidden variable h_j with a coupling W_{nj}. After the time evolution $e^{-\delta_\tau \mathcal{H}_{lm}^{\text{bond}}}$, as shown schematically in Fig. 3(c), the coupling parameters are updated in the following way based on the old W_{nj}: First, the first deep unit $d_{[l]}$ becomes coupled to the already existing hidden variables h_j through the coupling $W'_{j[l]}$ given in Eq. (173). The second deep unit $d_{[lm]}$ becomes similarly coupled to h_j through a term Z_{lmj} given in Eq. (173). Second, W_{nj} is updated to $\bar{W}_{nj} = W_{nj} + \Delta W_{nj}$ [see Eq. (172)]. Third, newly introduced $h_{[n]}$ ($n = l$ or m) gets coupled to $d_{[l]}$ through $W'_{[n][l]}$, and also to σ_n^z through $W_{n[n]}$ [Eqs. (179), (181)].

Within this construction, and as clarified in Methods, we also need to satisfy the constraint $d_{[l]}d_{[lm]} = \sigma_l^z \sigma_m^z$. Such a constraint is represented in DBM form as

$$\sum_{h_{[lm1]}, h_{[lm2]}} \exp[\frac{i\pi}{4}(h_{[lm1]}+h_{[lm2]})(\sigma_l^z + \sigma_m^z + d_{[l]} + d_{[lm]})],$$

(13)

which ensures $d_{[l]}d_{[lm]} = \sigma_l^z \sigma_m^z$ after explicit summation of $h_{[lm1]}$ and $h_{[lm2]}$.

Finally, we remark that the three constructions presented here have different intrinsic network topologies. In particular, 2d-6h gives rise to a local topology (because of the equivalence with the path-integral contruction), 1d-3h has a local structure in the first layer and non-local in the second one, and 2d-4h is purely non-local in both layers (see Supplementary Information II.B).

SAMPLING STRATEGIES

With network structures explicitly determined, we now focus on the problem of extracting meaningful physical quantities from them. To this end, it is convenient to decompose the DBM weight into two parts, such that

$$\Psi_{\mathcal{W}}(\sigma^z) = \sum_{\{h,d\}} P_1(\sigma^z, h)P_2(h, d),$$

(14)

where $P_1(\sigma^z, h) = e^{\sigma^z \cdot a + \sigma^z \cdot W \cdot h + h \cdot b}$, and $P_2(h, d) = e^{h \cdot W' \cdot d + d \cdot b'}$. The expectation value of an arbitrary (few-body) operator $\mathcal{O}$ can then be computed through the expression

$$\langle \mathcal{O} \rangle = \frac{\sum_{\{\sigma^z, h, h', d, d'\}} \Pi(\sigma^z, h, h', d, d') O_{\text{loc}}(\sigma^z, h, h')}{\sum_{\{\sigma^z, h, h', d, d'\}} \Pi(\sigma^z, h, h', d, d')}$$

(15)

where we have introduced the pseudo-probability density $\Pi(\sigma^z, h, h', d, d') \equiv P_1(\sigma^z, h)P_2(h, d)P_1^\star(\sigma^z, h')P_2^\star(h', d')$,

and the "local" estimator $O_{\text{loc}}(\sigma^z, h, h') = \frac{1}{2}\sum_{\sigma'z} \langle \sigma^z | \mathcal{O} | \sigma'^z \rangle \left(\frac{P_1(\sigma'^z, h)}{P_1(\sigma^z, h)} + \frac{P_1(\sigma'^z, h')^\star}{P_1(\sigma^z, h')^\star} \right)$.

For the sampling over the Π distribution, a block Gibbs sampling analogous to what performed in standard DBM architectures can be performed [37, 39]. Alternatively, it is possible to devise a set of Metropolis local updates sampling the exactly known marginals $\tilde{\Pi}(\sigma^z, h, h') = \sum_{\{d,d'\}} \Pi(\sigma^z, h, h', d, d')$ or $\tilde{\Pi}'(\sigma^z, d, d') = \sum_{\{h,h'\}} \Pi(\sigma^z, h, h', d, d')$. We can also employ efficient cluster updates. Sampling is discussed more in detail in the Supplementary Information (III).

NUMERICAL RESULTS

We have implemented numerical algorithms to sample and obtain physical properties from the DBM previously derived. In Fig. 4 (a) we show results for the one-dimensional TFI model. Specifically, we show the expectation value of the energy following the imaginary-time evolution starting from a fully polarized (in the x direction) initial state. The initial state corresponds to an empty network, where all the DBM parameters are set to zero. The DBM results closely match the exact imaginary-time evolution, thus verifying the correctness of our construction.

Numerical results for the one-dimensional Heisenberg model are shown in Figure 4 (b-c). Specifically, 4(b) shows the numerical check for the DBM (construction 2d-6h) time evolution for one-dimensional Heisenberg model for $N = 16$. As expected, the DBM results also in this case follow the exact time evolution. Figure 4(c) shows the dependence of the energy from the initial state, for $N = 80$ case. Specifically, by taking a pre-optimized variational RBM as an initial state as an initial state, we can significantly decrease the time τ needed to reach the ground state.

In the case of the TFI model, sampling from the DBM is realized through the Gibbs scheme previously sketched, in conjunction with a parallel tempering scheme, to improve ergodicity in the sampling. In the AFH model with 2d-6h representation, we employ loop update [40] used in the path-integral QMC method, because the imaginary-time evolution in the 2d-6h representation has a direct correspondence to the path-integral formulation, allowing for an efficient handling of the constraint $d_{[l]} + d_{[m]} = \sigma_l^z + \sigma_m^z$.

DISCUSSION

We have shown how exact ground states of interacting spin Hamiltonians can be explicitly constructed using artificial neural networks comprising only two layers of hidden variables. In contrast to approaches based on
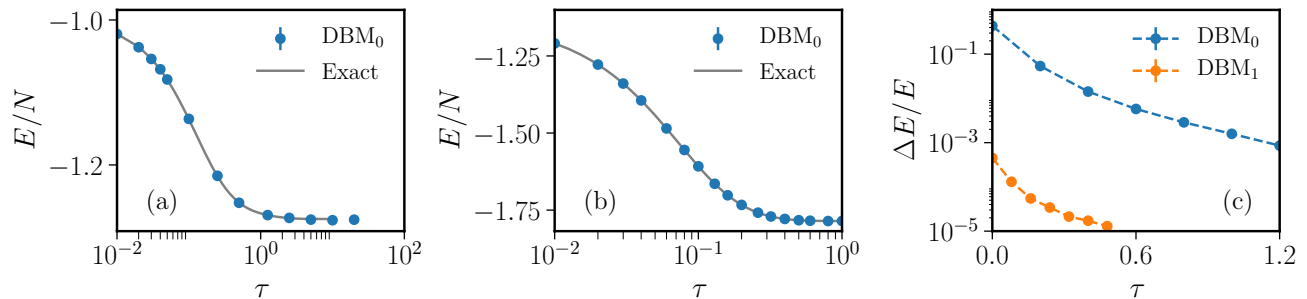
Figure 4. **Imaginary-time evolution with a DBM for 1D spin models**. (a) Expectation value of energy of the transverse-field Ising Hamiltonian in the exact imaginary-time evolution (continuous line) is compared to the stochastic result obtained with a DBM ($J\delta_\tau = 0.01$). We consider the critical point ($\Gamma_l = 1$), periodic boundary conditions, and $N = 20$ sites. (b) Expectation value of the isotropic antiferromagnetic Heisenberg Hamiltonian (AFHM) in the exact imaginary-time evolution (continuous line) is compared to the stochastic result obtained with a DBM ($J\delta_\tau = 0.01$) following 2d-6h construction. We consider periodic boundary conditions, $N = 16$ sites. (c) Relative error on the ground-state energy for the 1D AFHM as a function of the imaginary time. Here we consider periodic boundary conditions, $N = 80$ sites, and $J\delta_\tau = 0.01$. The subscript α in DBM$_\alpha$ in panels (a,b,c) specifies a different initial state $|\Psi_0\rangle$: $\alpha = 1$ means that the initial state is an RBM state with hidden-unit density $M/N = 1$, whereas when $\alpha = 0$ the initial state is the empty-network state ($M = 0$).

one-layer RBMs, the constructions we have derived here do not require further variational optimization of the network parameters. In the case of the Heisenberg model, all of the explicit algorithms presented here give rise to sign-problem-free representations, if the lattice is bipartite. The DBM representation has an intrinsic conceptual value, as an alternative to the path-integral representation. Notably, the additional deep hidden layer in the DBM plays a similar role as an additional dimension in statistical mechanics. Whereas a single layer (RBM) is enough to describe exactly the state of a classical system [see Eq. (23)], a second layer is necessary to describe exactly quantum mechanical states.

DBM-based schemes can be further used to systematically improve upon existing RBM variational results. More generally, the initial state for the present DBM scheme can be generic variational states or even combinations of RBMs and more conventional wave functions [24, 33]. We have shown that, by starting the DBM construction from a pre-optimized variational state, a fast convergence to the exact ground state is observed. In conjunction with very accurate initial RBM states, this kind of scheme opens the possibility of characterizing the ground state even in the case of non-bipartite lattices with frustration effects, exploiting the transient regime in which the sign problem can be still efficiently handled numerically, as for example discussed in Ref. [41].

METHODS

Useful identities

It is useful to introduce several identities, which can be used when more complicated interactions between the visible

spins σ^z, hidden variables h and deep variables d beyond the standard form Eq. (1) are needed. The first identity reads

$$e^{s_1 s_2 V} = C \sum_{s_3 = \pm 1} e^{s_1 s_3 \tilde{V}_1 + s_2 s_3 \tilde{V}_2} = 2C \cosh(s_1 \tilde{V}_1 + s_2 \tilde{V}_2). \tag{16}$$

with

$$C = \frac{1}{2} e^{-|V|} \tag{17}$$

$$\tilde{V}_1 = \frac{1}{2} \text{arcosh}(e^{2|V|}) \tag{18}$$

$$\tilde{V}_2 = \text{sgn}(V) \times \tilde{V}_1 \tag{19}$$

for Ising variables s_1 and s_2, and a real interaction V. This is a gadget for decomposing two-body interactions, and can be proven by examining all the cases of s_1 and s_2.

By taking s_1 and s_2 as visible (physical) variables σ^z and s_3 as a hidden variable h, the direct classical two-body interaction between physical variables [the leftmost part in Eq. (16)] is cut and instead mediated by the hidden neuron h. Furthermore, a direct interaction between σ^z and d can also be decomposed: In the following derivations for the DBM wave constructions, for convenience, we sometimes introduce the direct interaction between σ^z and d, which is not allowed in the DBM structure. However, by taking s_1 as a visible spin σ^z, s_2 as a deep variable d, and s_3 as a hidden variable h in Eq. (16), one can eliminate the direct interaction between σ^z and d and decompose it into the interaction mediated only by h with trade-off of the summation over the hidden variable h. With this trick, one can recover the standard DBM form in Eq. (1).

Another identity (decomposition of four-body interaction)

8

is

$$e^{s_1 s_2 s_3 s_4 V} = \frac{1}{4} \sum_{s_5,s_6,s_7} \exp\left[i\frac{\pi}{4}(s_5+s_6)(s_1+s_2+s_3+s_7)\right]$$
$$\times \exp(s_4 s_7 V)$$
$$= \sum_{s_7} \cos^2\left[\frac{\pi}{4}(s_1+s_2+s_3+s_7)\right]\exp(s_4 s_7 V)$$

(20)

for Ising variables s_i with $i=1,\cdots,4$. Although we have introduced complex couplings in the first line, each term in the summation in the second line of Eq. (73) is positive definite if V is real. The second line remains nonzero only if $s_1 s_2 = s_3 s_7$, which proves the identity. This identity with s_1 and s_2 as physical variables, s_4, s_5, and s_6 as hidden variables, and s_3 and s_7 as deep variables, reads

$$e^{\sigma_1 \sigma_2 d_1 h_1 V} = \frac{1}{4}\sum_{h_2,h_3,d_2}\exp\left[i\frac{\pi}{4}(h_2+h_3)(\sigma_1+\sigma_2+d_1+d_2)\right]$$
$$\times \exp(h_1 d_2 V),$$

(21)

Note that the right hand side fits the DBM structure.

General three-body and two-body interactions can also be represented by the two-body form just by putting some of $s_1,\cdots s_4$ as constants in Eq.(20). These could be used instead of Eq. (16), although we employ Eq. (16) in the formalism below for the decoupling of the two-body interaction.

Finally, we discuss the gadgets for decomposing general N-body classical interactions using complex bias term b_j in addition to the couplings W and W', whereas the gadgets Eqs. (16) and (21) are represented only by W and W' interactions. The gadget reads

$$e^{\sigma_1 \sigma_2 ... \sigma_N V} = C\cos^2\left(b+\frac{\pi}{4}\sum_{i=1}^{N}\sigma_i\right)$$

(22)

$$= \frac{C}{4}\sum_{h_1,h_2} e^{ib(h_1+h_2)} e^{i\frac{\pi}{4}(h_1+h_2)(\sigma_1+\sigma_2+...+\sigma_N)}$$

(23)

with

$$b = \arctan\left(e^{-V}\right) - \frac{\pi}{4}\mathrm{mod}(N,4),$$

(24)

$$C = \frac{1}{\cos\left(\arctan\left(e^{-V}\right)\right)\times\sin\left(\arctan\left(e^{-V}\right)\right)}.$$

(25)

This fact suggests that any classical partition function defined for Ising spins can be written exactly in terms of an RBM. Although the RBM is shown to be powerful in representing also the quantum states, there is no analytical way to map quantum states to the RBM and one must rely on numerical optimizations to get the RBM parameters. In the present study, we show analytical mappings from quantum states to the DBM, which has additional hidden layer. In the statistical mechanics, it is known that quantum systems with D dimension can be mapped on $(D+1)$-dimensional classical systems. Therefore, having additional hidden layer in neural network language is equivalent to acquiring additional dimension in statistical mechanics.

Transverse-Field Ising model

The solution of Eq.(8) is found in the following way. The left hand side of Eq.(8) can be rewritten by using the notation Eq.(14) as

$$\sum_{\{h,d\}} P_1(\sigma^z,h)P_2(h,d)\left[1+\tanh(\Gamma_l\delta_\tau)e^{-2\sigma_l^z\sum_j h_j W_{lj}}\right]$$
$$= C\Psi_{\bar{\mathcal{W}}}(\sigma^z).$$

(26)

We look for a solution by adding one deep neuron $d_{[l]}$ and creating new couplings $W'_{j[l]}$ to the existing hidden neurons h_j which are connected to σ_l^z. We also allow for changes in the existing interaction parameters. In particular we set the new couplings to be $\bar{W}_{lj} = W_{lj} + \Delta W_{lj}$, (with ΔW_{lj} to be determined). Moreover, we introduce one hidden neuron $h_{[l]}$ coupled to σ_l^z and $d_{[l]}$ through the interactions $W_{l[l]}$ and $W'_{[l][l]}$, respectively. If we trace out $h_{[l]}$, the hidden neuron $h_{[l]}$ mediates the interaction between σ_l^z and $d_{[l]}$ (denoted as $W''_{l[l]}$).

With this choice, we have (in the representation where $h_{[l]}$ is traced out):

$$\Psi_{\bar{\mathcal{W}}}(\sigma^z) = \sum_{\{h,d\}}\sum_{d_{[l]}} P_1(\sigma^z,h)P_2(h,d)$$
$$e^{\sigma_l^z \sum_j \Delta W_{lj}h_j + d_{[l]}\sum_j h_j W'_{j[l]} + \sigma_l^z d_{[l]}W''_{l[l]}}.$$

(27)

The equations to be verified are obtained considering the two possible values of $\sigma_l^z = \pm 1$:

$$e^{\sum_j h_j\left(\Delta W_{lj}+W'_{j[l]}\right)+W''_{l[l]}} + e^{\sum_j h_j\left(\Delta W_{lj}-W'_{j[l]}\right)-W''_{l[l]}}$$
$$= C\times\left(1+\tanh(\Gamma_l\delta_\tau)e^{-2\sum_j h_j W_{lj}}\right)$$

(28)

$$e^{\sum_j h_j\left(-\Delta W_{lj}+W'_{j[l]}\right)-W''_{l[l]}} + e^{\sum_j h_j\left(-\Delta W_{lj}-W'_{j[l]}\right)+W''_{l[l]}}$$
$$= C\times\left(1+\tanh(\Gamma_l\delta_\tau)e^{2\sum_j h_j W_{lj}}\right).$$

(29)

This equation has a solution from the requirement that the hidden unit interactions on the left and right hand sides match, thus we require

$$\Delta W_{lj} + W'_{j[l]} = -2W_{lj}$$

(30)

$$\Delta W_{lj} - W'_{j[l]} = 0,$$

(31)

and

$$W''_{l[l]} = \frac{\log\tanh(\Gamma_l\delta_\tau)}{2}.$$

(32)

Notice that when $\Gamma_l > 0$, $W''_{l[l]}$ is also real. By using Eq. (16) with the following replacement $s_1\to\sigma_l^z$, $s_2\to d_{[l]}$, $s_3\to h_{[l]}$, $V\to W''_{l[l]}$, $\tilde{V}_1\to W_{l[l]}$ and $\tilde{V}_2\to W'_{[l][l]}$, the last condition determines the real couplings $W_{l[l]}$ and $W'_{[l][l]}$ as Eqs.(10) and (11).

Heisenberg model

Here, we show the derivation for the general form of bond Hamiltonian allowing anisotropy and bond-disorder: $\mathcal{H}_{lm}^{\mathrm{bond}} = J_{lm}^{xy}(\sigma_l^x\sigma_m^x+\sigma_l^y\sigma_m^y)+J_{lm}^z\sigma_l^z\sigma_m^z$. In the case of the bipartite lattice and the antiferromagnetic exchange $J_{lm}^z, J_{lm}^{xy}>0$, we further apply a local gauge transformation by a π rotation

around the z axis in the spin space as $\sigma^x \to -\sigma^x$ and $\sigma^y \to -\sigma^y$ on one of the sublattices, which gives a $-$ sign for $\sigma_l^x \sigma_m^x$ and $\sigma_l^y \sigma_m^y$ interactions. This transformation is equivalent to taking

$$J_{lm}^{xy} \to -J_{lm}^{xy}. \tag{33}$$

The gauge transformation enables to design a DBM neural network with real couplings $\{W, W'\}$ except for those to put "constraint" on the values of deep neuron spins (see more detail about the constraint in the following sections). It ensures that the DBM algorithm has no negative sign problems.

In the case of the antiferromagnetic Heisenberg model after the gauge transformation on the bipartite lattice, we must solve, for each bond,

$$\delta_{\sigma_l^z, \sigma_m^z} e^{-\delta_\tau J_{lm}^z} \Psi_{\mathcal{W}}(\sigma^z) + (1 - \delta_{\sigma_l^z, \sigma_m^z}) e^{\delta_\tau J_{lm}^z}$$
$$(\Psi_{\mathcal{W}}(\sigma^z) \cosh(2J_{lm}^{xy}\delta_\tau) + \Psi_{\mathcal{W}}(\sigma_l^z \leftrightarrow \sigma_m^z) \sinh(2J_{lm}^{xy}\delta_\tau))$$
$$= C\langle \sigma^z | \Psi_{\bar{\mathcal{W}}} \rangle. \tag{34}$$

It is also useful to explicitly write the expression for the exchange term in the second line above:

$$\Psi_{\mathcal{W}}(\sigma^z) \cosh(2J_{lm}^{xy}\delta_\tau) + \Psi_{\mathcal{W}}(\sigma_l^z \leftrightarrow \sigma_m^z) \sinh(2J_{lm}^{xy}\delta_\tau)$$
$$= \sum_{\{h,d\}} P_1(\sigma^z, h) P_2(h, d) \Big[\cosh(2J_{lm}^{xy}\delta_\tau) +$$
$$\sinh(2J_{lm}^{xy}\delta_\tau) e^{(\sigma_m^z - \sigma_l^z) \sum_j h_j (W_{lj} - W_{mj})} \Big]. \tag{35}$$

In the following derivations, for the antiferromagnetic Hamiltonian ($J_{lm}^z, J_{lm}^{xy} > 0$) after the gauge transformation, we look for a solution with zero bias terms (a_i, b_j, $b_k' = 0$, $\forall i, j, k$). We can also derive a sign-problem free solution for the imaginary time evolution in the absence of the explicit gauge transformation by introducing a complex bias term a_i. Indeed, in the "2 deep, 4 hidden" representation, we will explicitly show that taking a specific set of complex bias term a_i on physical spins is equivalent to the gauge transformation, making a solution free from the sign problem.

In a way similar to the TFI model, solutions of Eq. (105) can be found by specifying the structure of the deep Boltzmann machine and the three examples are the following.

1d-3h construction

We assume the structure of the updated wave function (corresponding to Eq. (27) for the TFI model) to be

$$\Psi_{\bar{\mathcal{W}}}(\sigma^z) = \sum_{\{h,d\}} \sum_{\substack{d_{[lm]} = \pm 1 \\ d_{[lm]} = \sigma_l^z \text{ if } \sigma_l^z = \sigma_m^z}} P_1(\sigma^z, h) P_2(h, d)$$
$$e^{\sigma_l^z \sum_j \Delta W_{lj} h_j + d_{[lm]} \sum_j h_j W_{j[lm]}' + d_{[lm]} \sigma_l^z W_{l[lm]}'' + V_{[lm]} \sigma_l^z \sigma_m^z}. \tag{36}$$

Similarly to the case of the TFI model, a solution of Eq. (105) is given by

$$\Delta W_{lj} = -W_{lj} + W_{mj} \tag{37}$$
$$W_{j[lm]}' = W_{lj} - W_{mj}. \tag{38}$$

and

$$W_{l[lm]}'' = -(\log \tanh(2J_{lm}^{xy}\delta_\tau))/2 \tag{39}$$
$$V_{[lm]} = -(\log \cosh(2J_{lm}^{xy}\delta_\tau))/2 - J_{lm}^z \delta_\tau \tag{40}$$

Notice that the first condition is equivalent to cutting all connections from spin l to the hidden units and attaching the spin l to all the hidden units connected to spin m, with an interaction W_{mj}.

Although the terms proportional to $W_{l[lm]}''$ and V_{lm} do not satisfy the standard DBM form, they can be transformed to the DBM form by introducing new hidden neurons $h_{[lm1]}$ and $h_{[lm2]}$ [see the gadget Eq. (16)]:

$$e^{\sigma_l^z d_{[lm]} W_{l[lm]}''} = C_{[lm1]} \sum_{h_{[lm1]}} e^{\sigma_l^z h_{[lm1]} W_{l[lm1]} + h_{[lm1]} d_{[lm]} W_{[lm1][lm]}'},$$

with

$$W_{l[lm1]} = W_{[lm1][lm]}' = \frac{1}{2} \text{arcosh} \left(\frac{1}{\tanh(2J_{lm}^{xy}\delta_\tau)} \right). \tag{41}$$

Similarly, the coupling $V_{[lm]}$ is decomposed as

$$e^{\sigma_l^z \sigma_m^z V_{[lm]}} = C_{[lm2]} \sum_{h_{[lm2]}} e^{\sigma_l^z h_{[lm2]} W_{l[lm2]} + \sigma_m^z h_{[lm2]} W_{m[lm2]}},$$

with

$$W_{l[lm2]} = -W_{m[lm2]} = \frac{1}{2} \text{arcosh} \left(\cosh(2J_{lm}^{xy}\delta_\tau) e^{2J_{lm}^z \delta_\tau} \right). \tag{42}$$

Finally, as discussed in the main text, the constraint $d_{[lm]} = \sigma_l^z$ when $\sigma_l^z = \sigma_m^z$ can be satisfied by adding the third neuron $h_{[lm3]}$, introducing pure complex $i\pi/6$ couplings.

2d-6h construction

In this case, the form of the new wave function reads

$$\Psi_{\bar{\mathcal{W}}}(\sigma^z) = \sum_{\{h,d\}} \sum_{\substack{d_{[l]}, d_{[m]} \\ d_{[l]} + d_{[m]} = \sigma_l^z + \sigma_m^z}} P_1(\sigma^z, h) P_2(h, d)$$
$$e^{\sum_j \sum_{n=l,m} h_j (\Delta W_{nj} \sigma_n^z + W_{j[n]}' d_{[n]}) + \sum_{n=l,m} \sigma_n^z (W_{n[l]}'' d_{[l]} + W_{n[m]}'' d_{[m]})}. \tag{43}$$

A solution of Eq. (105) is given by

$$W_{j[l]}' = W_{lj}, \tag{44}$$
$$W_{j[m]}' = W_{mj}, \tag{45}$$
$$\Delta W_{lj} = -W_{lj}, \tag{46}$$
$$\Delta W_{mj} = -W_{mj}, \tag{47}$$

and

$$W_{l[l]}'' = W_{m[m]}'' = -\frac{J_{lm}^z \delta_\tau}{2} - \frac{1}{4} \log \sinh(2J_{lm}^{xy}\delta_\tau), \tag{48}$$
$$W_{l[m]}'' = W_{m[l]}'' = -\frac{J_{lm}^z \delta_\tau}{2} - \frac{1}{4} \log \cosh(2J_{lm}^{xy}\delta_\tau). \tag{49}$$

The direct interactions between $(\sigma_l^z, d_{[l]})$, $(\sigma_m^z, d_{[m]})$, $(\sigma_l^z, d_{[m]})$, and $(\sigma_m^z, d_{[l]})$, are mediated by $h_{[lm1]}, h_{[lm2]}, h_{[lm3]}$,

and $h_{[lm4]}$, respectively, as follows

$$e^{\sigma_l^z d_{[l]} W_{l[l]}''} = C_{[lm1]} \sum_{h_{[lm1]}} e^{\sigma_l^z h_{[lm1]} W_{l[lm1]} + h_{[lm1]} d_{[l]} W_{[lm1][l]}'},$$

$$e^{\sigma_m^z d_{[m]} W_{m[m]}''} = C_{[lm2]} \sum_{h_{[lm2]}} e^{\sigma_m^z h_{[lm2]} W_{m[lm2]} + h_{[lm2]} d_{[m]} W_{[lm2][m]}'},$$

$$e^{\sigma_l^z d_{[m]} W_{l[m]}''} = C_{[lm3]} \sum_{h_{[lm3]}} e^{\sigma_l^z h_{[lm3]} W_{l[lm3]} + h_{[lm3]} d_{[m]} W_{[lm3][m]}'},$$

$$e^{\sigma_m^z d_{[l]} W_{m[l]}''} = C_{[lm4]} \sum_{h_{[lm4]}} e^{\sigma_m^z h_{[lm4]} W_{m[lm4]} + h_{[lm4]} d_{[l]} W_{[lm4][l]}'}.$$

By applying the gadget Eq. (16), the new W and W' interactions are given by, for small δ_τ (such that $\frac{e^{-J_{lm}^z \delta_\tau}}{\sqrt{\sinh(2J_{lm}^{xy}\delta_\tau)}} > 1$),

$$W_{l[lm1]} = W_{[lm1][l]}' = W_{m[lm2]} = W_{[lm2][m]}'$$
$$= \frac{1}{2}\text{arcosh}\left(\frac{e^{-J_{lm}^z \delta_\tau}}{\sqrt{\sinh(2J_{lm}^{xy}\delta_\tau)}}\right) \quad (50)$$

and

$$W_{l[lm3]} = -W_{[lm3][m]}' = W_{m[lm4]} = -W_{[lm4][l]}'$$
$$= \frac{1}{2}\text{arcosh}\left(\sqrt{\cosh(2J_{lm}^{xy}\delta_\tau)} \times e^{J_{lm}^z \delta_\tau}\right). \quad (51)$$

Finally, the constraint $d_{[l]} + d_{[m]} = \sigma_l^z + \sigma_m^z$ can be put by introducing additionally two hidden neurons $h_{[lm5]}$ and $h_{[lm6]}$, and by introducing complex couplings

$$\sum_{h_{[lm5]}, h_{[lm6]}} e^{i\frac{\pi}{4}\left((\sigma_l^z + \sigma_m^z)h_{[lm5]} - h_{[lm5]}(d_{[l]} + d_{[m]})\right)}$$
$$\times e^{i\frac{\pi}{8}\left((\sigma_l^z + \sigma_m^z)h_{[lm6]} - h_{[lm6]}(d_{[l]} + d_{[m]})\right)} \quad (52)$$

This term gives interactions among $d_{[l]}$, $d_{[m]}$, σ_l^z and σ_m^z: $4\cos\left(\frac{\pi}{4}(\sigma_l^z + \sigma_m^z - d_{[l]} - d_{[m]})\right)\cos\left(\frac{\pi}{8}(\sigma_l^z + \sigma_m^z - d_{[l]} - d_{[m]})\right)$, which realize the constraint.

2d-4h construction

For this construction, we assume the following structure for the wave-function after the propagator:

$$\Psi_{\bar{W}}(\sigma^z) = \sum_{\{h,d\}} \sum_{d_{[l]}} P_1(\sigma^z, h) P_2(h, d) e^{\sum_{j,n=l,m} \sigma_n^z h_j \Delta W_{nj}}$$

$$\times e^{\sum_j h_j d_{[l]} W_{j[l]}' + \sum_{n=l,m} \sigma_n^z d_{[l]} W_{n[l]}'' + \sum_j \sigma_l^z \sigma_m^z h_j d_{[l]} Z_{lmj}}.$$

In this case, we also look for a solution for the bond operator without the gauge transformation. This shows that the introduction of a complex bias term a_i can play the same role as the gauge transformation. Then, we need to solve:

$$\delta_{\sigma_l^z, \sigma_m^z} e^{-\delta_\tau J_{lm}^z} \Psi_{\mathcal{W}}(\sigma^z) + (1 - \delta_{\sigma_l^z, \sigma_m^z})e^{\delta_\tau J_{lm}^z}$$
$$(\Psi_{\mathcal{W}}(\sigma^z)\cosh(2J_{lm}^{xy}\delta_\tau) - \Psi_{\mathcal{W}}(\sigma_l^z \leftrightarrow \sigma_m^z)\sinh(2J_{lm}^{xy}\delta_\tau))$$
$$= C\langle\sigma^z|\Psi_{\bar{W}}\rangle. \quad (53)$$

Note that the sign for $\Psi_{\mathcal{W}}(\sigma_l^z \leftrightarrow \sigma_m^z)\sinh(2J_{lm}^{xy}\delta_\tau)$ term is different from that in Eq. (105).

A solution of Eq. (53) is obtained as

$$\Delta W_{lj} = -\Delta W_{mj} = -\frac{1}{2}(W_{lj} - W_{mj}), \quad (54)$$

where W_{nj} ($n = l, m$) is updated to $\bar{W}_{nj}$ with the increment ΔW_{nj} as $\bar{W}_{nj} = W_{nj} + \Delta W_{nj}$. The new couplings $W_{j[l]}'$, Z_{lmj} and $W_{n[l]}'$ are also given by

$$W_{j[l]}' = -Z_{lmj} = -\frac{1}{2}(W_{lj} - W_{mj}) \quad (55)$$

and

$$W_{l[l]}'' = \frac{1}{4}\left[\log\left[-e^{-2a_{l-m}}\tanh(2J_{lm}^{xy}\delta_\tau)\right]\right.$$
$$\left. + 2\text{arcosh}\left[\frac{e^{-2J_{lm}^z \delta_\tau}}{\sqrt{-2e^{-2a_{l-m}}\sinh(4J_{lm}^{xy}\delta_\tau)}}\right]\right] \quad (56)$$

$$W_{m[l]}'' = \frac{1}{4}\left[-\log\left[-e^{-2a_{l-m}}\tanh(2J_{lm}^{xy}\delta_\tau)\right]\right.$$
$$\left. + 2\text{arcosh}\left[\frac{e^{-2J_{lm}^z \delta_\tau}}{\sqrt{-2e^{-2a_{l-m}}\sinh(4J_{lm}^{xy}\delta_\tau)}}\right]\right] \quad (57)$$

with $a_{l-m} = a_l - a_m$. On a bipartite lattice, to avoid the negative sign (or complex phase) problem we need to keep $W_{l[l]}''$ and $W_{m[l]}''$ real. This can be achieved by choosing $a_l = 0$ for any l if $J_{lm} < 0$ (ferromagnetic case). For $J_{lm} > 0$ (antiferromagnetic case), $a_l = n\pi i$ with an arbitrary integer n if the site l belongs to the sub-lattice A and $a_l = (n+1/2)\pi i$ if l belongs to the sub-lattice B. This local gauge for $J_{lm} > 0$ is equivalent to the transformation $J_{lm}^{xy} \to -J_{lm}^{xy}$ and $a_l = 0$ for any site l. We further notice that $W_{m[l]}''$ can be taken positive if we take a sufficiently small δ_τ in Eq (177), with the leading order term $-\log(2J_{lm}^{xy}\delta_\tau)/2$. On the other hand, in Eq. (176), the leading order term is negative ($= -J_{lm}\delta_\tau$).

To recover the original form of the DBM, we first use Eq. (16) with the replacement $s_1 \to \sigma_n^z$, $s_2 \to d_{[l]}$, $s_3 \to h_{[n]}$, $C \to D_n$, $V \to W_{n[l]}''$ $\tilde{V}_1 \to W_{n[n]}$ and $\tilde{V}_2 \to W_{[n][l]}'$ for $n = l, m$. Then a solution for D_n, $W_{n[n]}$, and $W_{[n][l]}'$ are represented by using $W_{n[l]}''$ as

$$D_n = \frac{1}{2}\exp[-W_{n[l]}''] \quad (58)$$

$$W_{n[n]} = W_{[n][l]}' = \frac{1}{2}\text{arcosh}(\exp[2W_{n[l]}'']), \quad (59)$$

for positive $W_{n[l]}''$ and

$$D_n = \frac{1}{2}\exp[W_{n[l]}''] \quad (60)$$

$$W_{n[n]} = -W_{[n][l]}' = \frac{1}{2}\text{arcosh}(\exp[-2W_{n[l]}'']), \quad (61)$$

for negative $W_{n[l]}''$ to give real $W_{n[n]}$ and $W_{[n][l]}'$.

To completely recover the original DBM form, we next use Eq. (21) by replacing σ_1 with σ_l^z, σ_2 with σ_m^z, d_1 with $d_{[l]}$, d_2 with $d_{[lm]}$, h_1 with h_j, h_2 with $h_{[lm1]}$, h_3 with $h_{[lm2]}$, and V with Z_{lmj}.

With these solutions, by ignoring the trivial constant factors including D_l and D_m, the evolution is described by introducing two deep and four hidden additional variables $d_{[l]}$,

$d_{[lm]}$, $h_{[l]}$, $h_{[m]}$, $h_{[lm1]}$, and $h_{[lm2]}$ as

$$\Psi_{\bar{\mathcal{W}}}(\sigma^z) = \sum_{\{\bar{h},\bar{d}\}} P_1(\sigma^z, h) P_2(h, d) \exp\Bigg[\sum_{j,n=l,m} \sigma_n^z h_j \Delta W_{nj}$$

$$+ \sum_j h_j d_{[l]} W'_{j[l]} + \sum_{n=l,m} h_{[n]}(\sigma_n^z W_{n[n]} + d_{[l]} W'_{[n][l]})$$

$$+ d_{[lm]} \sum_j h_j Z_{lmj} + \frac{i\pi}{4}(h_{[lm1]} + h_{[lm2]})(\sigma_l^z + \sigma_m^z + d_{[l]} + d_{[lm]}) \Bigg],$$

(62)

where $\{\bar{h}, \bar{d}\}$ is a set consisting of the existing and new neurons.

ACKNOWLEDGEMENTS

[1] Feynman, R. P. Space-Time Approach to Non-Relativistic Quantum Mechanics. *Reviews of Modern Physics* **20**, 367–387 (1948). URL https://link.aps.org/doi/10.1103/RevModPhys.20.367.

[2] Dyson, F. J. The S Matrix in Quantum Electrodynamics. *Physical Review* **75**, 1736–1755 (1949). URL https://link.aps.org/doi/10.1103/PhysRev.75.1736.

[3] Hubbard, J. Calculation of Partition Functions. *Physical Review Letters* **3**, 77–78 (1959). URL https://link.aps.org/doi/10.1103/PhysRevLett.3.77.

[4] Stratonovich, R. L. On a Method of Calculating Quantum Distribution Functions. *Soviet Physics Doklady* **2**, 416 (1957). URL http://adsabs.harvard.edu/abs/1957SPhD....2..416S.

[5] Abrikosov, A. A. *Methods of Quantum Field Theory in Statistical Physics* (Dover Publications, New York, 1975), revised edition edn.

[6] Binder, K. *Applications of the Monte Carlo Method in Statistical Physics* (Springer Verlag, Berlin, 1984).

[7] Takahashi, M. & Imada, M. Monte carlo calculation of quantum systems. *J. Phys. Soc. Jpn.* **53**, 963 (1984).

[8] Takahashi, M. & Imada, M. Monte carlo calculation of quantum systems. ii. higher order correction. *J. Phys. Soc. Jpn.* **53**, 3765 (1984).

[9] Ceperley, D. Path-Integrals in the Theory of Condensed Helium. *Reviews of Modern Physics* **67**, 279–355 (1995).

[10] Suzuki, M. Relationship between d-dimensional quantal spin systems and (d+1)-dimensional ising systems: Equivalence, critical exponents and systematic approximants of the partition function and spin correlations. *Prog. Theor. Phys.* **56**, 1454 (1976).

[11] Hirsch, J. E., Sugar, R., Scalapino, D. & Blankenbecler, R. Monte carlo simulations of one-dimensional fermion systems. *Phys. Rev. B* **26**, 5033 (1982).

[12] Beard, B. & Wiese, U.-J. Simulations of discrete quantum systems in continuous euclidean time. *J.Phys. Rev. Lett.* **77**, 5130 (1996).

[13] Sandvik, A. W. Stochastic series expansion method with operator-loop update. *Physical Review B* **59**, R14157–R14160 (1999). URL http://arxiv.org/abs/cond-mat/9902226. ArXiv: cond-mat/9902226.

[14] Prokof'ev, N. & Svistunov, B. Bold Diagrammatic Monte Carlo: When Sign Problem is Welcome. *Physical Review Letters* **99** (2007). URL http://arxiv.org/abs/cond-mat/0702555. ArXiv: cond-mat/0702555.

[15] Feynman, R. P. Atomic theory of the two-fluid model of liquid helium. *Physical Review* **94**, 262 (1954).

[16] Gros, C. Physics of projected wavefunctions. *Ann. Phys.* **189**, 53 (1989).

[17] Kashima, T. & Imada, M. Path-integral renormalization group method for numerical study on ground states of strongly correlated electronic systems. *J. Phys. Soc. Jpn.* **70**, 2287 (2001).

[18] Tahara, D. & Imada, M. Variational monte carlo method combined with quantum-number projection and multi-variable optimization. *J. Phys. Soc. Jpn.* **77**, 114701 (2008).

[19] Becca, F. & Sorella, S. *Quantum Monte Carlo Approaches for Correlated Systems* (Cambridge University Press, Cambridge, United Kingdom ; New York, NY, 2017).

[20] White, S. R. Density-matrix algorithms for quantum renormalization groups. *Physical Review B* **48**, 10345 (1993).

[21] Orús, R. A practical introduction to tensor networks: Matrix product states and projected entangled pair states. *Ann. Phys.* **349**, 117 (2014).

[22] Carleo, G. & Troyer, M. Solving the quantum many-body problem with artificial neural networks. *Science* **355**, 602–606 (2017). URL http://science.sciencemag.org/content/355/6325/602.

[23] Torlai, G. *et al.* Many-body quantum state tomography with neural networks. *arXiv:1703.05334* (2017). URL http://arxiv.org/abs/1703.05334. ArXiv: 1703.05334.

[24] Nomura, Y., Darmawan, A. S., Yamaji, Y. & Imada, M. Restricted boltzmann machine learning for solving strongly correlated quantum systems. *Phys. Rev. B* **96**, 205152 (2017).

[25] Deng, D.-L., Li, X. & Das Sarma, S. Quantum Entanglement in Neural Network States. *Physical Review X* **7**, 021021 (2017). URL https://link.aps.org/doi/10.1103/PhysRevX.7.021021.

[26] Rocchetto, A., Grant, E., Strelchuk, S., Carleo, G. & Severini, S. Learning hard quantum distributions with variational autoencoders. *arXiv:1710.00725 [quant-ph,*

stat] (2017). URL http://arxiv.org/abs/1710.00725. ArXiv: 1710.00725.

[27] Glasser, I., Pancotti, N., August, M., Rodriguez, I. D. & Cirac, J. I. Neural Networks Quantum States, String-Bond States and chiral topological states. *arXiv:1710.04045 [cond-mat, physics:quant-ph, stat]* (2017). URL http://arxiv.org/abs/1710.04045. ArXiv: 1710.04045.

[28] Kaubruegger, R., Pastori, L. & Budich, J. C. Chiral Topological Phases from Artificial Neural Networks. *arXiv:1710.04713 [cond-mat, physics:quant-ph]* (2017). URL http://arxiv.org/abs/1710.04713. ArXiv: 1710.04713.

[29] Cai, Z. Approximating quantum many-body wave-functions using artificial neural networks. *arXiv:1704.05148 [cond-mat]* (2017). URL http://arxiv.org/abs/1704.05148. ArXiv: 1704.05148.

[30] Saito, H. & Kato, M. Machine Learning Technique to Find Quantum Many-Body Ground States of Bosons on a Lattice. *Journal of the Physical Society of Japan* **87**, 014001 (2017). URL http://journals.jps.jp/doi/10.7566/JPSJ.87.014001.

[31] Saito, H. Solving the Bose–Hubbard Model with Machine Learning. *Journal of the Physical Society of Japan* **86**, 093001 (2017). URL http://journals.jps.jp/doi/10.7566/JPSJ.86.093001.

[32] Chen, J., Cheng, S., Xie, H., Wang, L. & Xiang, T. Equivalence of restricted Boltzmann machines and tensor network states. *Physical Review B* **97**, 085104 (2018). URL https://link.aps.org/doi/10.1103/PhysRevB.97.085104.

[33] Clark, S. R. Unifying Neural-network Quantum

States and Correlator Product States via Tensor Networks. *arXiv:1710.03545 [cond-mat, physics:quant-ph]* (2017). URL http://arxiv.org/abs/1710.03545. ArXiv: 1710.03545.

[34] Deng, D.-L., Li, X. & Das Sarma, S. Machine learning topological states. *Physical Review B* **96**, 195145 (2017). URL https://link.aps.org/doi/10.1103/PhysRevB.96.195145.

[35] Gao, X. & Duan, L.-M. Efficient representation of quantum many-body states with deep neural networks. *Nature Communications* **8**, 662 (2017). URL https://www.nature.com/articles/s41467-017-00705-2.

[36] Huang, Y. & Moore, J. E. Neural network representation of tensor network and chiral states. *arXiv:1701.06246* (2017). URL http://arxiv.org/abs/1701.06246. ArXiv: 1701.06246.

[37] Salakhutdinov, R. & Hinton, G. Deep Boltzmann Machines. In *PMLR*, 448–455 (2009). URL http://proceedings.mlr.press/v5/salakhutdinov09a.html.

[38] Trotter, H. F. On the product of semi-groups of operators. *Proc. Amer. Math. Soc.* **10**, 545 (1959).

[39] Salakhutdinov, R. & Hinton, G. An efficient learning procedure for deep Boltzmann machines. *Neural Computation* **24**, 1967–2006 (2012).

[40] Evertz, H. G., Lana, G. & Marcu, M. Cluster algorithm for vertex models. *Phys. Rev. Lett.* **70**, 875–879 (1993).

[41] Ceperley, D. M. & Alder, J. Ground state of the electron gas by a stochastic method. *Phys. Rev. Lett.* **45**, 566 (1980).

[42] Suzuki, M., Miyashita, S. & Kuroda, A. Monte carlo simulation of quantum spin systems. i. *Prog. Theor. Phys.* **58**, 1377–1387 (1977).

Supplementary Information

I. DEEP BOLTZMANN MACHINES

Deep Boltzmann machine representation of quantum states. In the main text we have considered a representation of the many-body wave-function in terms of a two-layers deep Boltzmann Machine (DBM). In the following we specialize to the case of N spin $1/2$ particles, described by the quantum numbers $|\sigma^z\rangle = |\sigma_1^z \dots \sigma_N^z\rangle$ with $\sigma_i^z = \pm 1$. Then, we represent the amplitudes $\langle \sigma_1^z \dots \sigma_N^z |\Psi\rangle \equiv \Psi(\sigma^z)$ in the DBM form:

$$\Psi_{\mathcal{W}}(\sigma^z) = \sum_{\{h\}} e^{\sum_i a_i \sigma_i^z} e^{\sum_{ij} \sigma_i^z h_j W_{ij} + \sum_j b_j h_j} \sum_{\{d\}} e^{\sum_{jk} h_j d_k W'_{jk} + \sum_k b'_k d_k}. \tag{63}$$

Here, we have introduced M hidden units h_j, M' deep units d_k, and a set of couplings and bias terms $\mathcal{W} \equiv (a, b, b', W, W')$. Hereafter, we call the neurons in the 1st hidden layer just hidden neurons and distinguish them from the neurons in the 2nd hidden layer, which are called deep neurons.

All those parameters, in general, must be taken complex-valued to represent a generic many-body state. The hidden and deep units are taken here to be of spin $1/2$, i.e. $h_j = \pm 1$, $d_k = \pm 1$, and the summations are over all the possible values of those variables. From a pictorial point of view, the DBM architecture features direct connections (interactions) between nearest-neighboring layers. In particular, the visible layer of physical degrees of freedom $(\sigma_1^z \dots \sigma_N^z)$ is connected only to the first layer of hidden variables $(h_1 \dots h_M)$, whereas the first layer is connected both to the visible spins and to the deep spins $(d_1 \dots d_{M'})$.

For the following derivations, it is useful to write the DBM amplitudes as:

$$\Psi_{\mathcal{W}}(\sigma^z) = \sum_{\{h,d\}} P_1(\sigma^z, h) P_2(h, d), \tag{64}$$

where we have introduced the two quantities:

$$P_1(\sigma^z, h) = e^{\sum_i a_i \sigma_i^z} e^{\sum_{ij} \sigma_i^z h_j W_{ij} + \sum_j b_j h_j} \tag{65}$$

$$P_2(h, d) = e^{\sum_{jk} h_j d_k W'_{jk} + \sum_k b'_k d_k}. \tag{66}$$

Notice that, in general, those weights are complex-valued, and cannot be interpreted as genuine Boltzmann weights. From these expressions, it is also straightforward to see that the Restricted Boltzmann Machine (RBM) expression for the wave-function is recovered when $M' = 0$, i.e. taking

$$\Psi_{\mathcal{W}}^{\text{RBM}}(\sigma^z) = \sum_{\{h\}} P_1(\sigma^z, h) \tag{67}$$

$$= e^{\sum_i a_i \sigma_i^z} \Pi_j^M 2 \cosh\left(\sum_i^N \sigma_i^z h_j W_{ij} + b_j \right), \tag{68}$$

where we have explicitly performed the summation of the hidden variables. At variance with the RBM case, in the more general case when $M' > 0$, it is not possible to analytically obtain the DBM amplitudes.

Useful gadgets in constructing DBM neural network. In the Methods we have discussed several useful identities to decompose spin interactions. In particular, those identities are very useful if we need more complicated interactions between the visible spins σ^z, hidden variables h and deep variables d beyond the standard form Eq. (63). For the sake of completeness of this Supplementary Information, we reproduce here the identities for decomposing two-body, three-body, and four-body interactions.

The first identity reads

$$e^{s_1 s_2 V} = C \sum_{s_3 = \pm 1} e^{s_1 s_3 \tilde{V}_1 + s_2 s_3 \tilde{V}_2} = 2C \cosh(s_1 \tilde{V}_1 + s_2 \tilde{V}_2). \tag{69}$$

with

$$C = \frac{1}{2} e^{-|V|} \tag{70}$$

$$\tilde{V}_1 = \frac{1}{2} \text{arcosh}(e^{2|V|}) \tag{71}$$

$$\tilde{V}_2 = \text{sgn}(V) \times \tilde{V}_1 \tag{72}$$

for Ising variables s_1 and s_2, and a real interaction V. This is the gadget for decomposing two-body interactions discussed in Methods. In the following, we will use this identity to decompose either interactions between visible (physical spins) (in that case s_1 and s_2 are both σ^z variables), or to decompose direct interactions between a σ^z spin and a deep unit d.

Another identity (decomposition of four-body interaction) is

$$
\begin{aligned}
e^{s_1 s_2 s_3 s_4 V} &= \frac{1}{4} \sum_{s_5, s_6, s_7} \exp\left[i\frac{\pi}{4}(s_5 + s_6)(s_1 + s_2 + s_3 + s_7)\right] \exp(s_4 s_7 V) \\
&= \sum_{s_7} \cos^2\left[\frac{\pi}{4}(s_1 + s_2 + s_3 + s_7)\right] \exp(s_4 s_7 V)
\end{aligned}
\tag{73}
$$

for Ising variables s_i with $i = 1, \cdots, 4$. Although we have introduced complex couplings in the first line, each term in the summation in the second line of Eq. (73) is positive definite if V is real. The second line remains nonzero only for $s_7 = 1$ if $s_1 s_2 s_3 = 1$ and only for $s_7 = -1$ if $s_1 s_2 s_3 = -1$, which proves the identity. This identity with s_1 and s_2 as physical variables, s_4, s_5, and s_6 as hidden variables, and s_3 and s_7 as deep variables, which reads

$$
e^{\sigma_1 \sigma_2 d_1 h_1 V} = \frac{1}{4} \sum_{h_2, h_3, d_2} \exp\left[i\frac{\pi}{4}(h_2 + h_3)(\sigma_1 + \sigma_2 + d_1 + d_2)\right] \exp(h_1 d_2 V),
\tag{74}
$$

will be used in Sec. II B 3. Note that the right hand side fits the DBM structure.

Although identities for decomposing three-body interactions are not used in the following derivation, it is nonetheless useful to show them:

$$
\begin{aligned}
e^{s_1 s_2 s_3 V} &= \frac{1}{4} \sum_{s_4, s_5, s_6} \exp\left[i\frac{\pi}{4}(s_4 + s_5)(s_1 + s_2 + s_3 + s_6)\right] \exp(s_6 V) \\
&= \sum_{s_6} \cos^2\left[\frac{\pi}{4}(s_1 + s_2 + s_3 + s_6)\right] \exp(s_6 V).
\end{aligned}
\tag{75}
$$

This gadget for three-body interactions is obtained by fixing $s_4 = 1$ in Eq. (73) (and changing variables). Alternative form is obtained by replacing s_3 with 1 in Eq. (73), which gives,

$$
\begin{aligned}
e^{s_1 s_2 s_3 V} &= \frac{1}{4} \sum_{s_4, s_5, s_6} \exp\left[i\frac{\pi}{4}(s_4 + s_5)(s_1 + s_2 + s_6 + 1)\right] \exp(s_3 s_6 V) \\
&= \sum_{s_6} \cos^2\left[\frac{\pi}{4}(s_1 + s_2 + s_6 + 1)\right] \exp(s_3 s_6 V).
\end{aligned}
\tag{76}
$$

As we see, the gadgets for three-body interactions [Eqs. (75) and (76)] have been derived from the gadget for four-body interactions [Eq. (73)] trivially.

Gadgets for two-body interactions which are different from Eq. (69) can also be obtained from Eq. (73) by fixing two variables out of s_1, s_2, s_3, s_4 to be 1. These could be used instead of (69), although we employ (69) in the formalism below for the decoupling of the two-body interaction.

II. REPRESENTING GROUND-STATES

As discussed in the main text, our goal is to construct explicit DBM representations of ground-states of local Hamiltonians. This goal is achieved by finding a representation of the imaginary-time evolved state:

$$
|\Psi(\tau)\rangle = e^{-\tau \mathcal{H}} |\Psi_0\rangle,
\tag{77}
$$

where $|\Psi_0\rangle$ is empty RBM ($\langle \sigma^z | \Psi_0 \rangle = \text{const.}$) or pre-optimized RBM state, converging to the exact ground-state for large enough τ. To achieve this goal we first consider a second-order Trotter-Suzuki decomposition:

$$
|\Psi(\tau)\rangle = \mathcal{G}_1(\delta_\tau/2)\mathcal{G}_2(\delta_\tau) \ldots \mathcal{G}_1(\delta_\tau)\mathcal{G}_2(\delta_\tau)\mathcal{G}_1(\delta_\tau/2)|\Psi_0\rangle,
\tag{78}
$$

where δ_τ is a small time step, the Hamiltonian is decomposed into two non-commuting parts, $\mathcal{H} = \mathcal{H}_1 + \mathcal{H}_2$, and $\mathcal{G}_\nu(\delta_\tau) = e^{-\mathcal{H}_\nu \delta_\tau}$ are short-time propagators. For given Hamiltonian, we then need to find specific rules to apply the short-time propagators to a generic DBM, and obtain a new (time-evolved) DBM, possibly with a larger total number of hidden and deep neurons. In the following, we show concrete examples for the transverse-field Ising and Heisenberg models.

A. Transverse-Field Ising model

Let us start with the case of the transverse-field Ising model. We consider a Trotter-Suzuki decomposition of the imaginary-time propagator, into two parts: $\mathcal{H}_1 = -\sum_i \Gamma_i \sigma_i^x$, and $\mathcal{H}_2 = \sum_{l<m} V_{lm}\sigma_l^z \sigma_m^z$. In the following derivation, we assume that Γ_i is positive ($\Gamma_i > 0$). In this case, we look for a solution with zero bias terms: $a_i = b_j = b'_k = 0$, $\forall i, j, k$. The case of negative Γ_i can also be treated, and is discussed more in detail at the end of this section.

Interaction propagator. The interaction propagator $e^{-\delta_\tau V_{lm}\sigma_l^z \sigma_m^z}$ is diagonal in the σ^z basis, and applying it to a DBM will lead to a modification in the DBM parameters. In particular, the goal is to satisfy the equation:

$$\langle \sigma^z | e^{-\delta_\tau V_{lm}\sigma_l^z \sigma_m^z} | \Psi_{\mathcal{W}} \rangle = C \langle \sigma^z | \Psi_{\bar{\mathcal{W}}} \rangle, \tag{79}$$

i.e. to explicitly find a set of parameters $\bar{\mathcal{W}}$ that satisfies the previous equation for all the possible $\langle \sigma^z |$, and for an arbitrary constant C.

We can achieve this goal adding a hidden unit in the first layer, $h_{[lm]}$ such that it is only connected to the visible spins: $W'_{[lm]k} = 0, \forall k$. The new wave function has then the form:

$$\Psi_{\bar{\mathcal{W}}}(\sigma^z) = \sum_{\{h,d\}} \sum_{h_{[lm]}} P_1(\sigma^z, h) P_2(h, d) e^{\sigma_l^z W_{l[lm]} h_{[lm]} + \sigma_m^z W_{m[lm]} h_{[lm]}} \tag{80}$$

$$= 2\cosh\left(\sigma_l^z W_{l[lm]} + \sigma_m^z W_{m[lm]}\right) \Psi_{\mathcal{W}}(\sigma^z). \tag{81}$$

Equation (79) is then satisfied if

$$e^{-\delta_\tau V_{lm}\sigma_l^z \sigma_m^z} = 2C \cosh\left(\sigma_l^z W_{l[lm]} + \sigma_m^z W_{m[lm]}\right) \tag{82}$$

for all the possible values of σ_l^z and σ_m^z. By using the gadget Eq. (69), the new parameters $W_{l[lm]}$ and $W_{m[lm]}$ are given by

$$W_{l[lm]} = \frac{1}{2}\text{arcosh}\left(e^{2|V_{lm}|\delta_\tau}\right) \tag{83}$$

$$W_{m[lm]} = -\text{sgn}(V_{lm}) \times W_{l[lm]}. \tag{84}$$

Transverse-field propagator. The propagator involving the transverse-field $e^{\delta_\tau \Gamma_l \sigma_l^x}$ is off-diagonal in σ^z basis. For this off-diagonal part, we must solve a slightly more involved equation:

$$\langle \sigma^z | e^{\delta_\tau \Gamma_l \sigma_l^x} | \Psi_{\mathcal{W}} \rangle = \Psi_{\mathcal{W}}(\sigma^z) \times \cosh(\Gamma_l \delta_\tau) + \Psi_{\mathcal{W}}(\sigma_1^z, \cdots - \sigma_l^z, \ldots, \sigma_N^z) \times \sinh(\Gamma_l \delta_\tau) \tag{85}$$

$$= C \langle \sigma^z | \Psi_{\bar{\mathcal{W}}} \rangle, \tag{86}$$

for the new parameters $\bar{\mathcal{W}}$, and for an arbitrary finite normalization constant C. In turn, this equation is equivalent to:

$$\sum_{\{h,d\}} P_1(\sigma^z, h) P_2(h, d) \left[1 + \tanh(\Gamma_l \delta_\tau) e^{-2\sigma_l^z \sum_j h_j W_{lj}}\right] = C\Psi_{\bar{\mathcal{W}}}(\sigma^z). \tag{87}$$

We look for a solution by adding one deep neuron $d_{[l]}$ and creating new couplings $W'_{j[l]}$ to the existing hidden neurons h_j which are connected to σ_l^z. We also allow for changes in the existing interaction parameters. In particular we set the new couplings to be $\bar{W}_{lj} = W_{lj} + \Delta W_{lj}$, (with ΔW_{lj} to be determined).

Moreover, we introduce one hidden neuron $h_{[l]}$ coupled to σ_l^z and $d_{[l]}$ through the interactions $W_{l[l]}$ and $W'_{[l][l]}$, respectively. If we trace out $h_{[l]}$, the hidden neuron $h_{[l]}$ mediates the interaction between σ_l^z and $d_{[l]}$ (denoted as $W''_{l[l]}$).

With this choice, we have (in the representation where $h_{[l]}$ is traced out):

$$\Psi_{\bar{\mathcal{W}}}(\sigma^z) = \sum_{\{h,d\}} \sum_{d_{[l]}} P_1(\sigma^z, h) P_2(h, d) e^{\sigma_l^z \sum_j \Delta W_{lj} h_j + d_{[l]} \sum_j h_j W'_{j[l]} + \sigma_l^z d_{[l]} W''_{l[l]}}. \tag{88}$$

The equations to be verified are obtained considering the two possible values of $\sigma_l^z = \pm 1$:

$$e^{\sum_j h_j \left(\Delta W_{lj} + W'_{j[l]}\right) + W''_{l[l]}} + e^{\sum_j h_j \left(\Delta W_{lj} - W'_{j[l]}\right) - W''_{l[l]}} = C \times \left(1 + \tanh(\Gamma_l \delta_\tau) e^{-2\sum_j h_j W_{lj}}\right) \tag{89}$$

$$e^{\sum_j h_j \left(-\Delta W_{lj} + W'_{j[l]}\right) - W''_{l[l]}} + e^{\sum_j h_j \left(-\Delta W_{lj} - W'_{j[l]}\right) + W''_{l[l]}} = C \times \left(1 + \tanh(\Gamma_l \delta_\tau) e^{2\sum_j h_j W_{lj}}\right). \tag{90}$$

This equation has a solution if the hidden unit interactions on the l.h.s. and on the r.h.s match, i.e. when:

$$\Delta W_{lj} + W'_{j[l]} = -2W_{lj} \tag{91}$$

$$\Delta W_{lj} - W'_{j[l]} = 0, \tag{92}$$

which in turn are verified when

$$W'_{j[l]} = -W_{lj} \tag{93}$$

$$\Delta W_{lj} = -W_{lj}, \tag{94}$$

and if

$$W''_{l[l]} = \frac{\log \tanh(\Gamma_l \delta_\tau)}{2}. \tag{95}$$

When $\Gamma_l > 0$, $W''_{l[l]}$ is real. By using Eq. (69) with the following replacement $s_1 \to \sigma_l^z$, $s_2 \to d_{[l]}$, $s_3 \to h_{[l]}$, $V \to W''_{l[l]}$, $\tilde{V}_1 \to W_{l[l]}$ and $\tilde{V}_2 \to W'_{[l][l]}$, the last condition determines the real couplings $W_{l[l]}$ and $W'_{[l][l]}$, which read

$$W_{l[l]} = \frac{1}{2}\text{arcosh}\left(\frac{1}{\tanh(\Gamma_l \delta_\tau)}\right) \tag{96}$$

$$W'_{[l][l]} = -W_{l[l]}. \tag{97}$$

Notice that because of condition (94), after applying the off-diagonal propagator all the interactions W_{lj} between spin l and hidden units h_j are set to zero. However, because of condition (96), the spin l is reconnected to the new hidden unit $h_{[l]}$ with the $W_{l[l]}$ interaction.

Negative transverse field. When $\Gamma_i < 0$, it is still possible to recover a DBM representation with purely real interaction weights W and W'. In order to do so, we apply the gauge transformation $\sigma_i^x \to -\sigma_i^x$ and $\sigma_i^y \to -\sigma_i^y$ (π spin rotation around the z axis), which maps onto the Hamiltonian with positive Γ_i. This gauge transformation can be achieved by taking a finite bias terms a_i in Eq. (63) as $a_i = i\pi/2$ and fix them during the imaginary time evolution. With this complex bias term $a_i = i\pi/2$, $|\uparrow\rangle$ ($|\downarrow\rangle$) state at the ith site acquires a phase as follows $|\uparrow\rangle \to e^{i\frac{\pi}{2}}|\uparrow\rangle = i|\uparrow\rangle$ ($|\downarrow\rangle \to e^{-i\frac{\pi}{2}}|\downarrow\rangle = -i|\downarrow\rangle$), which is equivalent to a π spin rotation around the z axis. In the case when Γ_i is originally positive, we can set all the bias terms $\{a, b, b'\}$ to be zero.

B. Heisenberg Model

We now consider the case of the Heisenberg model, whose Hamiltonian reads

$$\mathcal{H} = \sum_{\langle lm \rangle} \mathcal{H}_{lm} \tag{98}$$

$$\mathcal{H}_{lm} = \mathcal{H}_{lm}^z + \mathcal{H}_{lm}^{xy} \tag{99}$$

$$\mathcal{H}_{lm}^z = J_{lm}^z \sigma_l^z \sigma_m^z \tag{100}$$

$$\mathcal{H}_{lm}^{xy} = J_{lm}^{xy}(\sigma_l^x \sigma_m^x + \sigma_l^y \sigma_m^y) = 2J_{lm}^{xy}(\sigma_l^+ \sigma_m^- + \sigma_l^- \sigma_m^+) \tag{101}$$

with $J_{lm}^z = J_{lm}^{xy} = J$. We write the Hamiltonian in a general form because the following DBM algorithm can be straightforwardly extended to the more general case of anisotropic/disordered bonds. As a starting point for our construction, we decompose the Hamiltonian into pieces by a Trotter-Suzuki decomposition of the imaginary-time propagator: $e^{-\delta_\tau \mathcal{H}} \sim \prod_{\langle lm \rangle} e^{-\delta_\tau \mathcal{H}_{lm}} + O(\delta_\tau^2)$. Then in this Section, we represent $e^{-\delta_\tau \mathcal{H}_{lm}}$ by using the DBM in three different forms, which are all exact. By taking δ_τ small enough and operating $e^{-\delta_\tau \mathcal{H}_{lm}}$ many times, those constructions ensure that the ground state is obtained with any controlled accuracy.

For $e^{-\delta_\tau \mathcal{H}_{lm}}$, and the antiferromagnetic exchange $J_{lm}^z, J_{lm}^{xy} > 0$, if the lattice is bipartite, we further apply a local gauge transformation by π rotation around z axis in the spin space as

$$\sigma^x \to -\sigma^x \quad \text{and} \quad \sigma^y \to -\sigma^y \tag{102}$$

on one of the sublattices, which gives a $-$ sign for the $\sigma_l^x \sigma_m^x$ and $\sigma_l^y \sigma_m^y$ interactions. It is equivalent to the following transformation in the couplings:

$$J_{lm}^{xy} \to -J_{lm}^{xy}. \tag{103}$$

The gauge transformation enables to design a DBM neural network with real couplings $\{W, W'\}$ except for those necessary to enforce local constraints on the values of deep neuron spins (see more detail about the constraint in the following sections). Overall, we show in the following that the 3 different DBM constructions have no negative sign problem.

On the bipartite lattice, the Suzuki-Trotter decomposition is frequently expressed by decomposing the Hamiltonian $\mathcal{H}$ into several groups. For instance, on the one dimensional chain, if it is natural to decompose it into odd and even bonds:

$$\mathcal{H}_1 = \sum_{\langle l,m \rangle \in \text{odd bond}} \mathcal{H}_{lm}, \quad \mathcal{H}_2 = \sum_{\langle l,m \rangle \in \text{even bond}} \mathcal{H}_{lm}, \tag{104}$$

further decompositions $e^{-\delta_\tau \mathcal{H}_1} = \prod_{\langle l,m \rangle \in \text{ odd bond}} e^{-\delta_\tau \mathcal{H}_{lm}}$ and $e^{-\delta_\tau \mathcal{H}_2} = \prod_{\langle l,m \rangle \in \text{ even bond}} e^{-\delta_\tau \mathcal{H}_{lm}}$ contain commuting elements and are therefore exact. For the square lattice, a similar procedure requires the decomposition of the Hamiltonian into 4 parts, in a checkerboard fashion. In all cases, the fundamental ingredient to represent the ground-state as a DBM is to find an exact expression for the bond propagator, $e^{-\delta_\tau \mathcal{H}_{lm}}$, when applied to an existing DBM state.

In the case of antiferromagnetic Heisenberg model after the gauge transformation on the bipartite lattice, we must solve, for each bond,

$$\langle \sigma^z | e^{\delta_\tau J_{lm}^{xy} \left(\sigma_l^x \sigma_m^x + \sigma_l^y \sigma_m^y \right) - \delta_\tau J_{lm}^z \sigma_l^z \sigma_m^z} | \Psi_{\mathcal{W}} \rangle$$
$$= \delta_{\sigma_l^z, \sigma_m^z} e^{-\delta_\tau J_{lm}^z} \Psi_{\mathcal{W}}(\sigma^z) + (1 - \delta_{\sigma_l^z, \sigma_m^z}) e^{\delta_\tau J_{lm}^z} \left(\Psi_{\mathcal{W}}(\sigma^z) \times \cosh(2 J_{lm}^{xy} \delta_\tau) + \Psi_{\mathcal{W}}(\sigma_l^z \leftrightarrow \sigma_m^z) \times \sinh(2 J_{lm}^{xy} \delta_\tau) \right)$$
$$= C \langle \sigma^z | \Psi_{\bar{\mathcal{W}}} \rangle. \tag{105}$$

It is also useful to explicitly write the expression for the exchange term in the second line above:

$$\Psi_{\mathcal{W}}(\sigma^z) \times \cosh(2 J_{lm}^{xy} \delta_\tau) + \Psi_{\mathcal{W}}(\sigma_l^z \leftrightarrow \sigma_m^z) \times \sinh(2 J_{lm}^{xy} \delta_\tau)$$
$$= \sum_{\{h,d\}} P_1(\sigma^z, h) P_2(h, d) \left[\cosh(2 J_{lm}^{xy} \delta_\tau) + \sinh(2 J_{lm}^{xy} \delta_\tau) e^{(\sigma_m^z - \sigma_l^z) \sum_j h_j (W_{lj} - W_{mj})} \right]. \tag{106}$$

In the following derivations, for the antiferromagnetic Hamilonian ($J_{lm}^z, J_{lm}^{xy} > 0$) after the gauge transformation, we look for a solution with zero bias terms (a_i, b_j, $b'_k = 0$, $\forall i, j, k$). We can also derive a sign-problem free solution for the imaginary time evolution in the absence of the explicit gauge transformation by introducing complex bias term a_i. Indeed, in the "2 deep, 4 hidden" representation in Sec. II B 3, we will explicitly show that taking a specific set of complex bias term a_i on physical spins is equivalent to the gauge transformation, making a solution free from the sign problem.

1. 1 deep, 3 hidden (1d-3h) representation

Strategy. The first representation we propose is obtained adding one deep neuron $d_{[lm]}$, which gives new couplings $W'_{j[lm]}$ to the hidden units h_j connected to σ_l^z and σ_m^z. We also allow for changes in the existing DBM parameters. In particular we set the new couplings to be $\bar{W}_{lj} = W_{lj} + \Delta W_{lj}$, (with ΔW_{lj} to be determined). We introduce a coupling $W''_{l[lm]}$ between σ_l^z and $d_{[lm]}$, and a coupling $V_{[lm]}$ between σ_l^z and σ_m^z, which are both not allowed in the DBM architecture. By using the gadget Eq. (69), these interactions can be mediated by hidden neurons $h_{[lm1]}$ and $h_{[lm2]}$, respectively, and the DBM form is recovered. Furthermore, we look for a solution with a constraint: $d_{[lm]} = \sigma_l^z$ when $\sigma_l^z = \sigma_m^z$ (when $\sigma_l^z \neq \sigma_m^z$, the $d_{[lm]}$ value is not constrained). Imposing the constraint on the value of the deep unit is a crucial difference from the DBM solution for the TFI model. We will show that this constraint can be achieved by adding additional hidden neuron $h_{[lm3]}$ and introducing complex couplings ("$i\pi/6$" trick). We discuss this trick in more detail later.

In total, we introduce one deep and three hidden neurons. After tracing out the three hidden neurons $h_{[lm1]}$, $h_{[lm2]}$, and $h_{[lm3]}$, the new wave function reads

$$\Psi_{\bar{\mathcal{W}}}(\sigma^z) = \sum_{\{h,d\}} \sum_{\substack{d_{[lm]} = \pm 1 \\ d_{[lm]} = \sigma_l^z \text{ if } \sigma_l^z = \sigma_m^z}} P_1(\sigma^z, h) P_2(h, d) e^{\sigma_l^z \sum_j \Delta W_{lj} h_j + d_{[lm]} \sum_j h_j W'_{j[lm]} + d_{[lm]} \sigma_l^z W''_{l[lm]} + V_{[lm]} \sigma_l^z \sigma_m^z}. \tag{107}$$

Derivation for the update of parameters. The equations to be verified are then obtained considering all the possible values of $\sigma_l^z = \pm 1$ and $\sigma_m^z = \pm 1$, in addition to the constraints on $d_{[lm]}$ previously introduced. We then have two equations for $\sigma_l^z = \sigma_m^z = \pm 1$:

$$e^{\sum_j (\Delta W_{lj} + W'_{j[lm]})h_j + W''_{l[lm]} + V_{[lm]}} = C \times \exp(-J_{lm}^z \delta_\tau) \tag{108}$$

$$e^{\sum_j (-\Delta W_{lj} - W'_{j[lm]})h_j + W''_{l[lm]} + V_{[lm]}} = C \times \exp(-J_{lm}^z \delta_\tau), \tag{109}$$

and the other two equations for $\sigma_l^z = -\sigma_m^z = \pm 1$:

$$e^{\sum_j (\Delta W_{lj} + W'_{j[lm]})h_j + W''_{l[lm]} - V_{[lm]}} + e^{\sum_j (\Delta W_{lj} - W'_{j[lm]})h_j - W''_{l[lm]} - V_{[lm]}}$$
$$= C \times \exp(J_{lm}^z \delta_\tau) \left(\cosh(2J_{lm}^{xy}\delta_\tau) + \sinh(2J_{lm}^{xy}\delta_\tau)e^{-2\sum_j h_j(W_{lj} - W_{mj})} \right), \tag{110}$$

$$e^{\sum_j (-\Delta W_{lj} + W'_{j[lm]})h_j - W''_{l[lm]} - V_{[lm]}} + e^{\sum_j (-\Delta W_{lj} - W'_{j[lm]})h_j + W''_{l[lm]} - V_{[lm]}}$$
$$= C \times \exp(J_{lm}^z \delta_\tau) \left(\cosh(2J_{lm}^{xy}\delta_\tau) + \sinh(2J_{lm}^{xy}\delta_\tau)e^{2\sum_j h_j(W_{lj} - W_{mj})} \right). \tag{111}$$

These equations have a solution if the hidden unit interactions on the l.h.s. and on the r.h.s match, i.e. when:

$$\Delta W_{lj} + W'_{j[lm]} = 0 \tag{112}$$

$$\Delta W_{lj} - W'_{j[lm]} = -2(W_{lj} - W_{mj}) \tag{113}$$

which implies

$$\Delta W_{lj} = -W_{lj} + W_{mj} \tag{114}$$

$$W'_{j[lm]} = W_{lj} - W_{mj}. \tag{115}$$

Notice that the first condition gives $\bar{W}_{lj} = W_{lj} + \Delta W_{lj} = W_{mj}$, which is equivalent to cutting all connections from spin l to the hidden units and attaching the spin l to all the hidden units connected to spin m, with an interaction W_{mj}.

In order to match the coefficients we must also have:

$$W''_{l[lm]} + V_{[lm]} = \log C - J_{lm}^z \delta_\tau \tag{116}$$

$$W''_{l[lm]} - V_{[lm]} = \log C + \log \cosh(2J_{lm}^{xy}\delta_\tau) + J_{lm}^z \delta_\tau \tag{117}$$

$$-W''_{l[lm]} - V_{[lm]} = \log C + \log \sinh(2J_{lm}^{xy}\delta_\tau) + J_{lm}^z \delta_\tau, \tag{118}$$

which has the solution:

$$W''_{l[lm]} = -\left(\log \tanh(2J_{lm}^{xy}\delta_\tau) \right)/2 \tag{119}$$

$$V_{[lm]} = -\left(\log \cosh(2J_{lm}^{xy}\delta_\tau) \right)/2 - J_{lm}^z \delta_\tau \tag{120}$$

Recovery of standard DBM. The coupling $W''_{l[lm]}$ between the deep unit $d_{[lm]}$ and the visible spin σ_l^z is mediated by the hidden unit $h_{[lm1]}$ coupled to σ_l^z by $W_{l[lm1]}$ and $d_{[lm]}$ by $W'_{[lm1][lm]}$:

$$\exp(\sigma_l^z d_{[lm]} W''_{l[lm]}) = C_{[lm1]} \sum_{h_{[lm1]}} \exp(\sigma_l^z h_{[lm1]} W_{l[lm1]} + h_{[lm1]} d_{[lm]} W'_{[lm1][lm]}). \tag{121}$$

By using Eq. (69) with the following replacement $s_1 \to \sigma_l^z$, $s_2 \to d_{[lm]}$, $s_3 \to h_{[lm1]}$, $V \to W''_{l[lm]}$, $\tilde{V}_1 \to W_{l[lm1]}$ and $\tilde{V}_2 \to W'_{[lm1][lm]}$, $W_{l[lm1]}$ and $W'_{[lm1][lm]}$ are given by

$$W_{l[lm1]} = W'_{[lm1][lm]} = \frac{1}{2}\text{arcosh}\left(\frac{1}{\tanh(2J_{lm}^{xy}\delta_\tau)} \right). \tag{122}$$

Similarly, the coupling $V_{[lm]}$ between visible spins σ_l^z and σ_m^z is mediated by the hidden unit $h_{[lm2]}$ coupled to σ_l^z by $W_{l[lm2]}$ and σ_m^z by $W_{m[lm2]}$:

$$\exp(\sigma_l^z \sigma_m^z V_{[lm]}) = C_{[lm2]} \sum_{h_{[lm2]}} \exp(\sigma_l^z h_{[lm2]} W_{l[lm2]} + \sigma_m^z h_{[lm2]} W_{m[lm2]}). \tag{123}$$

By using Eq. (69) with the following replacement $s_1 \to \sigma_l^z$, $s_2 \to \sigma_m^z$, $s_3 \to h_{[lm2]}$, $V \to V_{lm}$, $\tilde{V}_1 \to W_{l[lm2]}$ and $\tilde{V}_2 \to W_{m[lm2]}$, $W_{l[lm2]}$ and $W_{m[lm2]}$ are given by

$$W_{l[lm2]} = -W_{m[lm2]} = \frac{1}{2}\mathrm{arcosh}\left(\cosh(2J_{lm}^{xy}\delta_\tau)e^{2J_{lm}^z \delta_\tau}\right). \tag{124}$$

How to enforce the constraint $d_{[lm]} = \sigma_l^z$ when $\sigma_l^z = \sigma_m^z$ ("$i\pi/6$" trick). The constraint $d_{[lm]} = \sigma_l^z$ when $\sigma_l^z = \sigma_m^z$ can be exactly satisfied by introducing pure complex connections. We can replace the sum with the constraint in Eq. (107) as follows (we ignore trivial constant factor):

$$\sum_{\substack{d_{[lm]}=\pm 1 \\ d_{[lm]}=\sigma_l^z \text{ if } \sigma_l^z=\sigma_m^z}} \longrightarrow \sum_{d_{[lm]}} \sum_{h_{[lm3]}} e^{i\frac{\pi}{6}\left((\sigma_l^z+\sigma_m^z)h_{[lm3]}-h_{[lm3]}d_{[lm]}\right)} = \sum_{d_{[lm]}} 2\cos\left(\frac{\pi}{6}\left(\sigma_l^z + \sigma_m^z - d_{[lm]}\right)\right) \tag{125}$$

One can easily see that the cosine term in the rightmost part gives nonzero value only when $d_{[lm]} = \sigma_l^z$ if $\sigma_l^z = \sigma_m^z$. On the other hand, if $\sigma_l^z \neq \sigma_m^z$, both $d_{[lm]} \pm 1$ contributions survive.

Proof of no negative sign. Here, we show that the marginal probability density $\tilde{\Pi}'(\sigma^z, d, d') = \sum_{h,h'} \Pi(\sigma^z, h, h', d, d')$ obtained by tracing out the hidden unit is non-negative definite. Therefore, we can perform the Metropolis sampling using $\tilde{\Pi}'$ density without suffering from the negative signs (see more detail on the sampling scheme in Sec. III B). To prove this, it is sufficient to show

$$\sum_{\{h\}} P_1(\sigma^z, h) P_2(h, d) \geq 0. \tag{126}$$

for all possible σ^z and d configurations.

In the 1d-3h representation, $i\pi/6$ complex couplings are originally introduced to put the constraint locally. However, as time evolves, these complex couplings become non-local (see Fig. 5). Because the pure complex couplings give cosine terms after tracing out hidden variables, they have a potential to give negative signs. Here, we prove that this is not the case.

We assume that Eq. (126) is satisfied for all possible σ^z and d after several steps of the imaginary time evolution. Then, we apply the bond propagator $e^{-\mathcal{H}_{lm}\delta_\tau}$ to obtain the new wave function. In the case when $\sigma_l^z = -\sigma_m^z = 1$, the solution in the 1d-3h representation can be rewritten as

$$\sum_{h_{[lm1]}, h_{[lm2]}, h_{[lm3]}} \bar{P}_1(\sigma^z, \bar{h}) \bar{P}_2(\bar{h}, d, d_{[lm]} = 1) = P_1(\sigma^z, h) P_2(h, d) \times (\text{positive constant}) \tag{127}$$

$$\sum_{h_{[lm1]}, h_{[lm2]}, h_{[lm3]}} \bar{P}_1(\sigma^z, \bar{h}) \bar{P}_2(\bar{h}, d, d_{[lm]} = -1) = P_1(\sigma_l^z \leftrightarrow \sigma_m^z, h) P_2(h, d) \times (\text{positive constant}) \tag{128}$$

where $\bar{P}_1 \times \bar{P}_2$ on the left hand side is the new weight after the imaginary time evolution, and $\{\bar{h}\}$ consists of the existing hidden neurons $\{h\}$ and the newly introduced hidden neurons $h_{[lm1]}$, $h_{[lm2]}$, and $h_{[lm3]}$. By taking the summation on the existing hidden variables on both sides, we get

$$\sum_{\{\bar{h}\}} \bar{P}_1(\sigma^z, \bar{h}) \bar{P}_2(\bar{h}, d, d_{[lm]} = 1) = \sum_{\{h\}} P_1(\sigma^z, h) P_2(h, d) \times (\text{positive constant}) \geq 0 \tag{129}$$

$$\sum_{\{\bar{h}\}} \bar{P}_1(\sigma^z, \bar{h}) \bar{P}_2(\bar{h}, d, d_{[lm]} = -1) = \sum_{\{h\}} P_1(\sigma_l^z \leftrightarrow \sigma_m^z, h) P_2(h, d) \times (\text{positive constant}) \geq 0 \tag{130}$$

Here, we used Eq. (126) to obtain the rightmost inequality. It proves that the new weight with the hidden variables being traced out is also non-negative. In the same way, we can show the non-negativeness of the new weight for $\sigma_l = -\sigma_m = -1$.
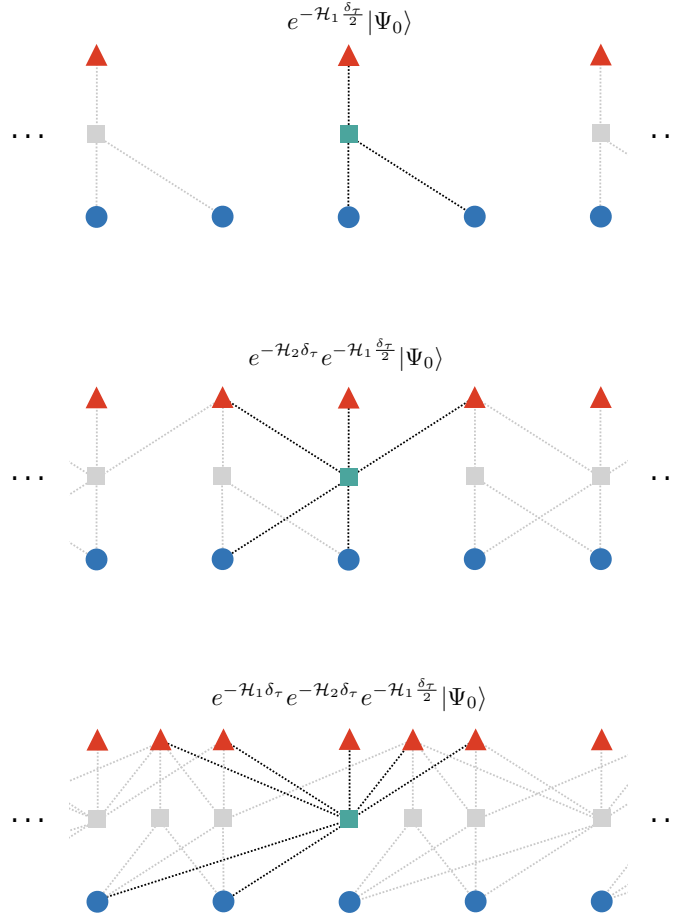
Figure 5. **Imaginary-time evolution of complex couplings in 1d-3h construction for one-dimensional Heisenberg model.** The figure shows how the complex couplings with weight $\pm i\pi/6$ evolve from an empty RBM ($\langle\sigma^z|\Psi_0\rangle = $ const.). Dots, squares, triangles indicate physical spins σ_i^z, hidden neurons h_j, and deep neurons d_k, respectively. For visibility, only hidden neurons having complex couplings and the associated complex couplings are shown. Therefore, at each imaginary-time evolution, one hidden neuron (called $h_{[lm3]}$ in the text) appears for each bond. One hidden neuron (green) and the associated couplings (black) are highlighted. As discussed in Step 2 in Fig. 3, at each evolution on σ_l^z and σ_m^z, the W couplings to σ_l^z are cut and σ_l^z is reconnected to the hidden neuron coupled to σ_m^z. By this "cut and reconnect" procedure, the positions of nonzero W couplings from a specific hidden neuron move, however, the W couplings stay local. On the other hand, the number of nonzero W' couplings increases by imaginary-time evolution, resulting in non-local structure of W' couplings. For the same reason, the real W couplings stay local, whereas the real W' couplings become nonlocal.

Next we consider the case $\sigma_l^z = \sigma_m^z = 1$. In this case,

$$\sum_{h_{[lm1]},h_{[lm2]},h_{[lm3]}} \bar{P}_1(\sigma^z, \bar{h})\bar{P}_2(\bar{h}, d, d_{[lm]} = 1) = P_1(\sigma^z, h)P_2(h, d) \times \text{(positive constant)}, \tag{131}$$

$$\sum_{h_{[lm1]},h_{[lm2]},h_{[lm3]}} \bar{P}_1(\sigma^z, \bar{h})\bar{P}_2(\bar{h}, d, d_{[lm]} = -1) = 0. \tag{132}$$

By taking the summation on the existing hidden variables on both sides, we obtain

$$\sum_{\{\bar{h}\}} \bar{P}_1(\sigma^z, \bar{h})\bar{P}_2(\bar{h}, d, d_{[lm]} = 1) = \sum_{h} P_1(\sigma^z, h)P_2(h, d) \times \text{(positive constant)} \geq 0 \tag{133}$$

$$\sum_{\{\bar{h}\}} \bar{P}_1(\sigma^z, \bar{h})\bar{P}_2(\bar{h}, d, d_{[lm]} = -1) = 0. \tag{134}$$

Therefore, the non-negativeness of the weight is ensured. The proof for $\sigma_l^z = \sigma_m^z = -1$ case can be done in an analogous way.

We have proven that the new weight after applying the bond propagator $e^{-\mathcal{H}_{lm}\delta_\tau}$ is non negative for all the possible σ^z and $\bar{d}$ configurations:

$$\sum_{\{\bar{h}\}} \bar{P}_1(\sigma^z, \bar{h})\bar{P}_2(\bar{h}, \bar{d}) \geq 0 \tag{135}$$

with $\{\bar{d}\}$ consisting of $\{d\}$ and $d_{[lm]}$. It ensures the non-negativeness of the weight at any time during the imaginary time evolution.

Summary of 1d-3h representation. The action the bond propagator is summarized as follows. First, the new deep neuron $d_{[lm]}$ is attached to the existing hidden neurons connected to σ_l^z and σ_m^z. Second, σ_l^z is disconnected to all hidden units and reconnected to the hidden units having finite couplings to σ_m^z ($\bar{W}_{lj} = W_{mj}$). Third, four couplings are inserted, involving new hidden neurons $h_{[lm1]}$ and $h_{[lm2]}$: $\sigma_l^z \leftrightarrow h_{[lm1]}$, $h_{[lm1]} \leftrightarrow d_{[l]}$, $\sigma_l^z \leftrightarrow h_{[lm2]}$ and $\sigma_m^z \leftrightarrow h_{[lm2]}$, Finally, the new hidden neuron $h_{[lm3]}$ puts the constraint on the $d_{[l]}$ sum by the imaginary couplings to σ_l^z, σ_m^z, and $d_{[l]}$.

By successively applying the imaginary-time evolutions, the W' couplings become nonlocal or long ranged. On the other hand, the W couplings stay local (see Fig. 5).

<center>2. 2 deep, 6 hidden (2d-6h) representation</center>

Strategy. We look for a solution where we add two deep neurons $d_{[l]}$ and $d_{[m]}$, giving new couplings $W'_{j[l]}$, $W'_{j[m]}$ to the existing hidden spins h_j connected to σ_l^z and σ_m^z. We also allow for changes in the existing W parameters: We set the new couplings to be $\bar{W}_{lj} = W_{lj} + \Delta W_{lj}$ and $\bar{W}_{mj} = W_{mj} + \Delta W_{mj}$ (with ΔW_{lj}, ΔW_{mj} to be determined). Furthermore, we add four hidden neurons $h_{[lm1]}$, $h_{[lm2]}$, $h_{[lm3]}$, and $h_{[lm4]}$ to mediate the interactions between $(\sigma_l^z, d_{[l]})$, $(\sigma_m^z, d_{[m]})$, $(\sigma_l^z, d_{[m]})$, and $(\sigma_m^z, d_{[l]})$, respectively. We solve the equation with the constraint $\sigma_l^z + \sigma_m^z = d_{[l]} + d_{[m]}$. This constraint can be achieved, for example, by adding two further hidden neurons ($h_{[lm5]}$ and $h_{[lm6]}$, respectively) and introducing complex connections ("$i\pi/4, i\pi/8$" trick). This trick will be discussed in detail later.

In total, we add two deep neurons ($d_{[l]}$ and $d_{[m]}$) and six hidden neurons ($h_{[lm1]}, \ldots, h_{[lm6]}$). In the following, to make equations simple, we employ a representation in which the new hidden neurons are analytically traced out. The interactions between $(\sigma_l^z, d_{[l]})$, $(\sigma_m^z, d_{[m]})$, $(\sigma_l^z, d_{[m]})$, and $(\sigma_m^z, d_{[l]})$, which are mediated by 1st to 4th hidden neurons, will be denoted as $W''_{l[l]}$, $W''_{m[m]}$, $W''_{l[m]}$, and $W''_{m[l]}$, respectively. The 5th and 6th hidden neurons filter out $\sigma_l^z + \sigma_m^z \neq d_{[l]} + d_{[m]}$ contributions. With this setting, the new wave function is represented as

$$\Psi_{\bar{\mathcal{W}}}(\sigma^z) = \sum_{\{h,d\}} \sum_{\substack{d_{[l]}, d_{[m]} \\ d_{[l]} + d_{[m]} = \sigma_l^z + \sigma_m^z}} P_1(\sigma^z, h) P_2(h, d)\ e^{\sum_j h_j(\Delta W_{lj}\sigma_l^z + W'_{j[l]}d_{[l]}) + \sum_j h_j(\Delta W_{mj}\sigma_m^z + W'_{j[m]}d_{[m]})}$$
$$\times\ e^{\sigma_l^z(W''_{l[l]}d_{[l]} + W''_{l[m]}d_{[m]}) + \sigma_m^z(W''_{m[l]}d_{[l]} + W''_{m[m]}d_{[m]})}. \tag{136}$$

Derivation for the update of parameters. When the lth and mth physical spins are anti-parallel ($\sigma_l^z = -\sigma_m^z = \pm 1$), $d_{[l]} = -d_{[m]} = \pm 1$ contributions survive in the sum over $d_{[l]}$ and $d_{[m]}$ variables in Eq. (136), and thus the equations to be satisfied are

$$e^{\sum_j h_j(\Delta W_{l-m,j} + W'_{j[l]} - W'_{j[m]}) + W''_{l-m,[l]} - W''_{l-m,[m]}} + e^{\sum_j h_j(\Delta W_{l-m,j} - W'_{j[l]} + W'_{j[m]}) - W''_{l-m,[l]} + W''_{l-m,[m]}}$$
$$= Ce^{J_{lm}^z\delta_\tau}\left(\cosh(2J_{lm}^{xy}\delta_\tau) + \sinh(2J_{lm}^{xy}\delta_\tau)e^{-2\sum_j h_j W_{l-m,j}}\right) \tag{137}$$

for $\sigma_l^z = -\sigma_m^z = 1$ and

$$e^{\sum_j h_j(-\Delta W_{l-m,j} + W'_{j[l]} - W'_{j[m]}) - W''_{l-m,[l]} + W''_{l-m,[m]}} + e^{\sum_j h_j(-\Delta W_{l-m,j} - W'_{j[l]} + W'_{j[m]}) + W''_{l-m,[l]} - W''_{l-m,[m]}}$$
$$= Ce^{J_{lm}^z\delta_\tau}\left(\cosh(2J_{lm}^{xy}\delta_\tau) + \sinh(2J_{lm}^{xy}\delta_\tau)e^{2\sum_j h_j W_{l-m,j}}\right) \tag{138}$$

for $\sigma_l^z = -\sigma_m^z = -1$, respectively. Here, $W_{l-m,[\alpha]} = W_{l[\alpha]} - W_{m[\alpha]}$, $\Delta W_{l-m,[\alpha]} = \Delta W_{l[\alpha]} - \Delta W_{m[\alpha]}$, $W''_{l-m,[\alpha]} = W''_{l[\alpha]} - W''_{m[\alpha]}$ with $\alpha = l, m$.

When the lth and mth physical spins are parallel ($\sigma_l^z = \sigma_m^z = \pm 1$), only $d_{[l]} = d_{[m]} = \sigma_l^z = \sigma_m^z$ contribution survives in the sum over $d_{[l]}$ and $d_{[m]}$ variables in Eq. (136), and thus the equations to be satisfied are

$$e^{\sum_j h_j \left(\Delta W_{l+m,j} + W'_{j[l]} + W'_{j[m]} \right) + W''_{l+m,[l]} + W''_{l+m,[m]}} = C e^{-J_{lm}^z \delta_\tau} \tag{139}$$

for $\sigma_l^z = \sigma_m^z = 1$

$$e^{\sum_j h_j \left(-\Delta W_{l+m,j} - W'_{j[l]} - W'_{j[m]} \right) + W''_{l+m,[l]} + W''_{l+m,[m]}} = C e^{-J_{lm}^z \delta_\tau} \tag{140}$$

for $\sigma_l^z = \sigma_m^z = -1$, respectively. Here, $W_{l+m,[\alpha]} = W_{l[\alpha]} + W_{m[\alpha]}$, $\Delta W_{l+m,[\alpha]} = \Delta W_{l[\alpha]} + \Delta W_{m[\alpha]}$, $W''_{l+m,[\alpha]} = W''_{l[\alpha]} + W''_{m[\alpha]}$ with $\alpha = l, m$.

The equations (137), (138), (139), and (140) are satisfied if

$$\Delta W_{l-m,j} - W'_{j[l]} + W'_{j[m]} = -2 W_{l-m,j}, \tag{141}$$

$$\Delta W_{l-m,j} + W'_{j[l]} - W'_{j[m]} = 0, \tag{142}$$

$$\Delta W_{l+m,j} + W'_{j[l]} + W'_{j[m]} = 0, \tag{143}$$

and

$$W''_{l-m,[l]} - W''_{l-m,[m]} = \log C + J_{lm}^z \delta_\tau + \log \cosh(2 J_{lm}^{xy} \delta_\tau), \tag{144}$$

$$-W''_{l-m,[l]} + W''_{l-m,[m]} = \log C + J_{lm}^z \delta_\tau + \log \sinh(2 J_{lm}^{xy} \delta_\tau), \tag{145}$$

$$W''_{l+m,[l]} + W''_{l+m,[m]} = \log C - J_{lm}^z \delta_\tau. \tag{146}$$

These conditions give

$$W'_{j[l]} = W_{lj}, \tag{147}$$

$$W'_{j[m]} = W_{mj}, \tag{148}$$

$$\Delta W_{lj} = -W_{lj}, \tag{149}$$

$$\Delta W_{mj} = -W_{mj}, \tag{150}$$

and

$$W''_{l[l]} = W''_{m[m]} = -\frac{J_{lm}^z \delta_\tau}{2} - \frac{1}{4} \log \sinh(2 J_{lm}^{xy} \delta_\tau), \tag{151}$$

$$W''_{l[m]} = W''_{m[l]} = -\frac{J_{lm}^z \delta_\tau}{2} - \frac{1}{4} \log \cosh(2 J_{lm}^{xy} \delta_\tau). \tag{152}$$

Recovery of standard DBM. The direct interactions between $(\sigma_l^z, d_{[l]})$, $(\sigma_m^z, d_{[m]})$, $(\sigma_l^z, d_{[m]})$, and $(\sigma_m^z, d_{[l]})$, are mediated by $h_{[lm1]}$, $h_{[lm2]}$, $h_{[lm3]}$, and $h_{[lm4]}$, respectively, as follows

$$\exp(\sigma_l^z d_{[l]} W''_{l[l]}) = C_{[lm1]} \sum_{h_{[lm1]}} \exp(\sigma_l^z h_{[lm1]} W_{l[lm1]} + h_{[lm1]} d_{[l]} W'_{[lm1][l]}), \tag{153}$$

$$\exp(\sigma_m^z d_{[m]} W''_{m[m]}) = C_{[lm2]} \sum_{h_{[lm2]}} \exp(\sigma_m^z h_{[lm2]} W_{m[lm2]} + h_{[lm2]} d_{[m]} W'_{[lm2][m]}), \tag{154}$$

$$\exp(\sigma_l^z d_{[m]} W''_{l[m]}) = C_{[lm3]} \sum_{h_{[lm3]}} \exp(\sigma_l^z h_{[lm3]} W_{l[lm3]} + h_{[lm3]} d_{[m]} W'_{[lm3][m]}), \tag{155}$$

$$\exp(\sigma_m^z d_{[l]} W''_{m[l]}) = C_{[lm4]} \sum_{h_{[lm4]}} \exp(\sigma_m^z h_{[lm4]} W_{m[lm4]} + h_{[lm4]} d_{[l]} W'_{[lm4][l]}). \tag{156}$$

By applying the gadget Eq. (69), the new W, W' interactions are given by, for small δ_τ (such that $\frac{e^{-J_{lm}^z \delta_\tau}}{\sqrt{\sinh(2 J_{lm}^{xy} \delta_\tau)}} > 1$):

$$W_{l[lm1]} = W'_{[lm1][l]} = W_{m[lm2]} = W'_{[lm2][m]} = \tfrac{1}{2} \text{arcosh} \left(\frac{e^{-J_{lm}^z \delta_\tau}}{\sqrt{\sinh(2 J_{lm}^{xy} \delta_\tau)}} \right), \tag{157}$$

$$W_{l[lm3]} = -W'_{[lm3][m]} = W_{m[lm4]} = -W'_{[lm4][l]} = \tfrac{1}{2} \text{arcosh} \left(\sqrt{\cosh(2 J_{lm}^{xy} \delta_\tau)} \times e^{J_{lm}^z \delta_\tau} \right). \tag{158}$$

How to enforce the constraint $\sigma_l^z + \sigma_m^z = d_{[l]} + d_{[m]}$ ("$i\pi/4, i\pi/8$" trick). Here, we discuss how to design the network to satisfy the constraint $\sigma_l^z + \sigma_m^z = d_{[l]} + d_{[m]}$. We rewrite the sum with the constraint in Eq. (136) as follows (we ignore trivial constant factor):

$$
\sum_{\substack{d_{[l]}, d_{[m]} \\ d_{[l]}+d_{[m]}=\sigma_l^z+\sigma_m^z}} \longrightarrow \sum_{d_{[l]}, d_{[m]}} \sum_{h_{[lm5]}, h_{[lm6]}} e^{i\frac{\pi}{4}\left((\sigma_l^z+\sigma_m^z)h_{[lm5]} - h_{[lm5]}(d_{[l]}+d_{[m]})\right)} \times e^{i\frac{\pi}{8}\left((\sigma_l^z+\sigma_m^z)h_{[lm6]} - h_{[lm6]}(d_{[l]}+d_{[m]})\right)}
$$

$$
= \sum_{d_{[l]}, d_{[m]}} 2\cos\left(\frac{\pi}{4}(\sigma_l^z + \sigma_m^z - d_{[l]} - d_{[m]})\right) \times 2\cos\left(\frac{\pi}{8}(\sigma_l^z + \sigma_m^z - d_{[l]} - d_{[m]})\right) \quad (159)
$$

One can easily see that the second line of the equation gives nonzero contribution only when $d_{[l]} + d_{[m]} = \sigma_l^z + \sigma_m^z$.

Summary of the 2d-6h representation. The network changes induced by the bond propagator at each imaginary time step are summarized as follows. Eqs. (149) and (150) imply that $\bar{W}_{lj} = W_{lj} + \Delta W_{lj} = 0$ and $\bar{W}_{mj} = W_{mj} + \Delta W_{mj} = 0$, i.e., all the existing connections between physical spins and hidden neurons vanish. Then, the lth and mth physical spins will be connected to the new hidden neurons $h_{[lm1]}, \ldots, h_{[lm6]}$, The new deep neurons $d_{[l]}$ and $d_{[m]}$ are also connected to $h_{[lm1]}, \ldots, h_{[lm6]}$. In total, we have 16 new connections in the deep Boltzmann network.

By continuing the imaginary time evolution, the neural network grows as in Fig. 6. The number of neurons increases linearly with the number N_{slice} of Suzuki-Trotter time slice. For example, in the case of the one-dimensional Heisenberg model, the total number of deep and hidden neurons are $N_{\text{site}}(2N_{\text{slice}} + 1)$ and $3N_{\text{site}}(2N_{\text{slice}} + 1)$, respectively. The number of nonzero connections in the network is $8N_{\text{site}}(2N_{\text{slice}} + 1)$. The origin of $2N_{\text{slice}} + 1$ is coming from the fact that we apply $\mathcal{G}$ propagators $2N_{\text{slice}} + 1$ times when we apply the second-order Suzuki-Trotter decomposition. The "$i\pi/4, i\pi/8$" trick plays a role to preserve the total magnetization for deep spins at each imaginary-time step, i.e., $\sum_k d_k(t+1) = \sum_k d_k(t)$, where $d(t+1)$ [$d(t)$] are the deep neurons introduced at $(t+1)$-th [t-th] step.

Relationship between the 2d-6h representation and the path-integral quantum Monte Carlo method. In the final part of this section, we discuss the similarity between the 2d-6h representation and the imaginary-time path-integral quantum Monte Carlo method [42]. We will show that, in the 2d-6h representation, the deep neurons can be regard as the additional degrees of freedom along the imaginary time in the path-integral formulation.

In the quantum Monte Carlo simulations using Suzuki-Trotter decomposition [10, 38], the partition function Z is evaluated as

$$
Z = \langle \sigma^z(0)|e^{-\beta\mathcal{H}}|\sigma^z(0)\rangle
$$
$$
\simeq \sum_{\sigma^z(0),\ldots,\sigma^z(2N_{\text{slice}}-1)} \langle \sigma^z(0)|e^{-\mathcal{H}_2\delta_\tau}|\sigma^z(2N_{\text{slice}}-1)\rangle\langle\sigma^z(2N_{\text{slice}}-1)|e^{-\mathcal{H}_1\delta_\tau}|\sigma^z(2N_{\text{slice}}-2)\rangle \ldots
$$
$$
\ldots \langle\sigma^z(4)|e^{-\mathcal{H}_2\delta_\tau}|\sigma^z(3)\rangle\langle\sigma(3)|e^{-\mathcal{H}_1\delta_\tau}|\sigma^z(2)\rangle\langle\sigma^z(2)|e^{-\mathcal{H}_2\delta_\tau}|\sigma^z(1)\rangle\langle\sigma^z(1)|e^{-\mathcal{H}_1\delta_\tau}|\sigma^z(0)\rangle
$$

$$(160)$$

In the evaluation of the matrix element of $\langle\sigma^z(t+1)|e^{-\mathcal{H}_\nu\delta_\tau}|\sigma^z(t)\rangle$ ($\nu = 1$ or 2), in the case of one-dimensional Heisenberg model, it is sufficient to consider one specific bond, $\langle\sigma_l^z(t+1)\sigma_m^z(t+1)|e^{-\mathcal{H}_{lm}\delta_\tau}|\sigma_l^z(t)\sigma_m^z(t)\rangle$. The matrix elements are given by

$$
\langle\sigma_l^z(t+1)\sigma_m^z(t+1)|e^{-\mathcal{H}_{lm}\delta_\tau}|\sigma_l^z(t)\sigma_m^z(t)\rangle = e^{J_{lm}^z\delta_\tau} \begin{pmatrix} e^{-2J_{lm}^z\delta_\tau} & 0 & 0 & 0 \\ 0 & \cosh(2J_{lm}^{xy}\delta_\tau) & \sinh(2J_{lm}^{xy}\delta_\tau) & 0 \\ 0 & \sinh(2J_{lm}^{xy}\delta_\tau) & \cosh(2J_{lm}^{xy}\delta_\tau) & 0 \\ 0 & 0 & 0 & e^{-2J_{lm}^z\delta_\tau} \end{pmatrix} \quad (161)
$$

in the basis $\{|\uparrow\uparrow\rangle, |\uparrow\downarrow\rangle, |\downarrow\uparrow\rangle, |\downarrow\downarrow\rangle\}$.

On the other hand, the imaginary time evolution in Eq. (2) in the main text [or equivalently, Eq. (78)] can be
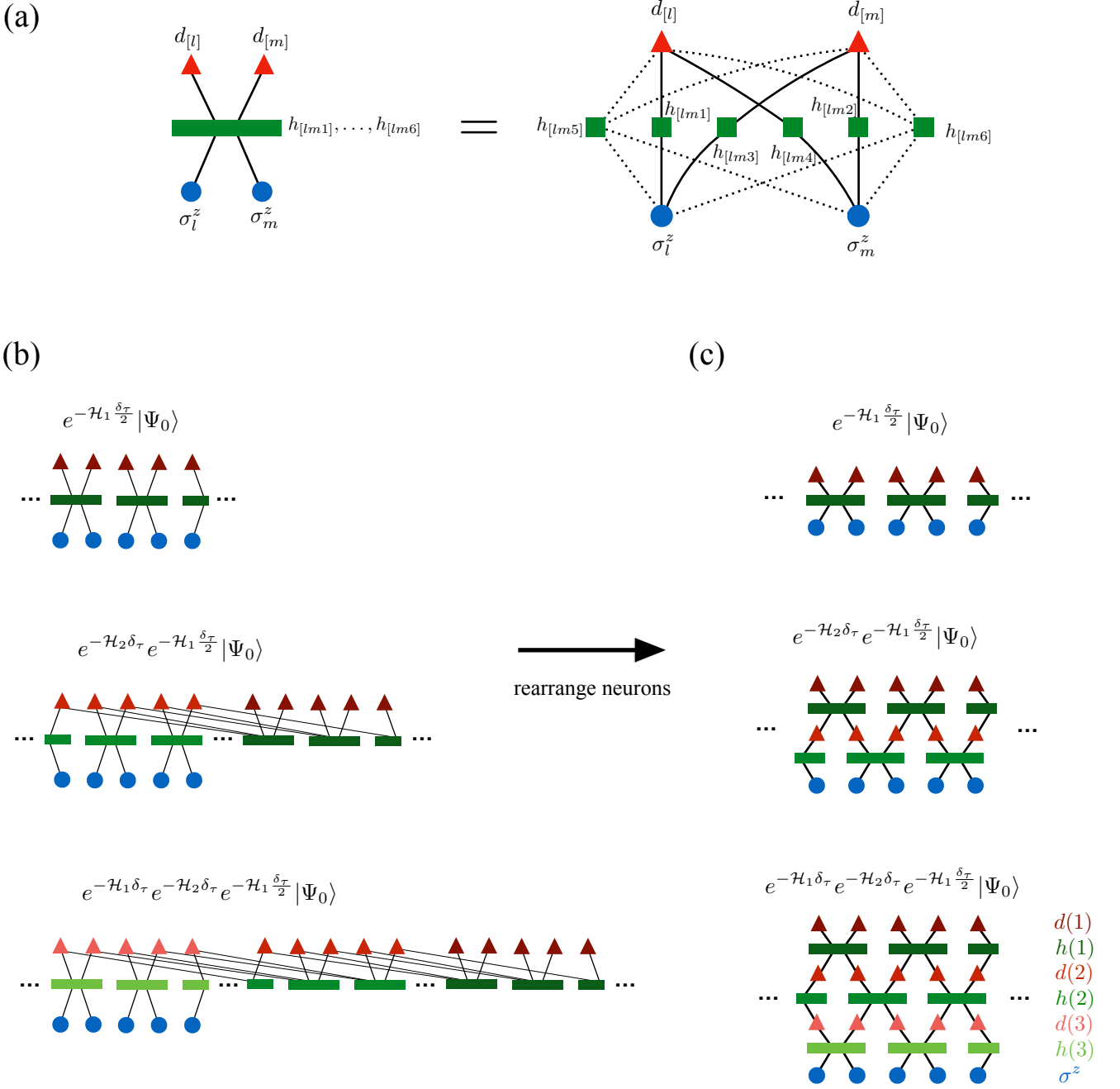
Figure 6. **Schematic picture for imaginary time evolution of DBM neural network in the 2d-6h construction.** Dots, squares, and triangles indicate physical spins σ_i^z, hidden neurons h_j, and deep neurons d_k, respectively. A set of six hidden neurons are depicted as rectangles. (a) Building block of the imaginary-time evolution. The left part is a simplified picture of the complete figure in the right part. This simplified picture is used in the panels (b) and (c) for the sake of visibility. (b) The imaginary time evolution of the network starting from an empty RBM ($\langle \sigma^z | \Psi_0 \rangle = $ const.). The hidden neurons introduced at t-th step ($h(t)$'s) lose their connections to physical spins at $(t+1)$-th step, and instead they get connections to $(t+1)$-th deep neurons ($d(t+1)$'s). (c) When we rearrange the neurons, one can see a clear correspondence between the 2d-6h representation and the path-integral formulation (see the text for detail).

rewritten as

$$\langle\sigma^z|\Psi(\tau)\rangle = \sum_{\sigma^z(1),\ldots,\sigma^z(2N_{\text{slice}}+1)} \langle\sigma^z|e^{-\mathcal{H}_1\frac{\delta_\tau}{2}}|\sigma^z(2N_{\text{slice}}+1)\rangle\langle\sigma^z(2N_{\text{slice}}+1)|e^{-\mathcal{H}_2\delta_\tau}|\sigma^z(2N_{\text{slice}})\rangle\ldots$$

$$\ldots\langle\sigma^z(4)|e^{-\mathcal{H}_1\delta_\tau}|\sigma^z(3)\rangle\langle\sigma^z(3)|e^{-\mathcal{H}_2\delta_\tau}|\sigma^z(2)\rangle\langle\sigma^z(2)|e^{-\mathcal{H}_1\frac{\delta_\tau}{2}}|\sigma^z(1)\rangle\langle\sigma^z(1)|\Psi_0\rangle \quad (162)$$

by inserting complete basis sets at each time slice. The matrix element used here is exactly the same as that of QMC in Eq. (161). Here, the D dimensional quantum spin system is mapped on the $D+1$ dimensional classical system as in the case of the path integral quantum Monte Carlo method. Because the neuron spins are defined as the classical Ising-type spins, we can represent the summation over $\sigma^z(1),\ldots,\sigma^z(2N_{\text{slice}}+1)$ by the summation over $N_{\text{site}}(2N_{\text{slice}}+1)$ neuron spins. Assuming that these $N_{\text{site}}(2N_{\text{slice}}+1)$ neuron spins are in the deep layer, the imaginary time evolution in Eq. (162) reads

$$\langle\sigma^z|\Psi(\tau)\rangle = \sum_{d(1),\ldots,d(2N_{\text{slice}}+1)} \langle\sigma^z|e^{-\mathcal{H}_1\frac{\delta_\tau}{2}}|d(2N_{\text{slice}}+1)\rangle\langle d(2N_{\text{slice}}+1)|e^{-\mathcal{H}_2\delta_\tau}|d(2N_{\text{slice}})\rangle\ldots$$

$$\ldots\langle d(4)|e^{-\mathcal{H}_1\delta_\tau}|d(3)\rangle\langle d(3)|e^{-\mathcal{H}_2\delta_\tau}|d(2)\rangle\langle d(2)|e^{-\mathcal{H}_1\frac{\delta_\tau}{2}}|d(1)\rangle\langle d(1)|\Psi_0\rangle. \quad (163)$$

The matrix element $\langle d_l(t+1)d_m(t+1)|e^{-\mathcal{H}_{lm}\delta_\tau}|d_l(t)d_m(t)\rangle$ can be reproduced, for example, by the following interaction

$$e^{W_1''(d_l(t+1)d_l(t)+d_m(t+1)d_m(t))}e^{W_2''(d_l(t+1)d_m(t)+d_m(t+1)d_l(t))}$$

$$\times \cos\left(\frac{\pi}{4}\left(d_l(t+1)+d_m(t+1)-d_l(t)-d_m(t)\right)\right)\cos\left(\frac{\pi}{8}\left(d_l(t+1)+d_m(t+1)-d_l(t)-d_m(t)\right)\right) \quad (164)$$

with

$$W_1'' = -\frac{J_{lm}^z\delta_\tau}{2} - \frac{1}{4}\log\sinh(2J_{lm}^{xy}\delta_\tau), \quad (165)$$

$$W_2'' = -\frac{J_{lm}^z\delta_\tau}{2} - \frac{1}{4}\log\cosh(2J_{lm}^{xy}\delta_\tau), \quad (166)$$

This interaction can be mediated by adding hidden neurons and mediating the interactions between $d(t+1)$ and $d(t)$. Then, Eq. (160) can be mapped onto the DBM representation.

Indeed, the 2d-6h representation presented in this section correspond to this specific DBM construction: In the 2d-6h representation, two deep neurons are introduced for each bond at each imaginary time evolution. Because each imaginary time evolution acts on either even or odd bonds, the number of deep neurons introduced at one step is exactly same as the number of physical spins. In this case, the deep neurons can be considered as the spin degrees of freedom in the imaginary time layers $d(1),\ldots,d(2N_{\text{slice}}+1)$. The interactions in Eqs. (165) and (166) are equivalent to those in Eqs. (151) and (152). The "$i\pi/4, i\pi/8$" trick appears to put constraint to conserve the total magnetization at each layer. Therefore, the 2d-6h representation is equivalent to the path-integral formulation. Indeed, if we rearrange the neurons in this DBM construction (Fig. 6), one can see a clear correspondence between the DBM network and the path-integral formulation. The extended systems including physical spins and deep neurons can be regard as the $D+1$ dimensional classical spin systems mapped from D dimensional quantum systems.

3. 2 deep, 4 hidden *(2d-4h)* representation

Strategy. We first extend DBM in the following way:

$$\Psi_{\bar{\mathcal{W}}}(\sigma^z) = \sum_{\{h,d\}}\sum_{d_{[l]}} P_1(\sigma^z,h)P_2(h,d)e^{\sum_{j,n=l,m}\sigma_n^z h_j \Delta W_{nj} + \sum_j h_j d_{[l]}W_{j[l]}' + \sum_{n=l,m}\sigma_n^z d_{[l]}W_{n[l]}'' + \sum_j \sigma_l^z\sigma_m^z h_j d_{[l]} Z_{lmj}}.$$

$$(167)$$

Here, we have introduced terms which break the standard DBM form, in particular the terms proportional to $W_{n[l]}''$ and Z_{lmj} with $n=l,m$. Those are essential for this construction, and their reduction to the pure DBM will be shown later. Also notice that the sum over j runs through all the hidden neuron sites coupled to σ_l^z and σ_m^z, thus it incorporates nonlocal couplings between hidden variables (h), physical (σ^z) and deep (d) variables. The term proportional to a_i in $P_1(\sigma^z,h)$ is a local site-dependent magnetic-field term in the DBM acting on the physical variables σ^z, which can also

flexibly represent any local gauge transformation, if a_i is taken complex. Here we fix a_i to be site-dependent constants, which stay unchanged through the imaginary time evolution. We later use the fact that the gauge transformation $\sigma^x \to -\sigma^x$ and $\sigma^y \to -\sigma^y$ on one of the sublattices (or $J^{xy} \to -J^{xy}$) on a bipartite lattice as in Eq. (103) is equivalent to $a_i = i\pi/2$ if i is on this sublattice and $a_i = 0$ on the other sublattice as a special choice of a_i.

In the imaginary time evolution of $\mathcal{H}_{lm}$, we update $\bar{W}_{nj}$ $(n = l, m)$ with the increment ΔW_{nj}, in such a way that $\bar{W}_{nj} = W_{nj} + \Delta W_{nj}$. In addition to the deep variable $d_{[l]}$, we further introduce one additional deep variable $d_{[lm]}$ to recover the standard DBM by transforming the term proportional to W'' and Z, with supplementary four hidden variables.

Derivation for the update of parameters. For $\sigma_l^z \sigma_m^z = -1$, the imaginary time evolution of the bond $\mathcal{H}_{lm}$ is given as

$$\langle \sigma^z | e^{-\delta_\tau (J_{lm}^z \sigma_l^z \sigma_m^z + 2J_{lm}^{xy}(\sigma_l^+ \sigma_m^- + \sigma_l^- \sigma_m^+))} | \Psi_{\mathcal{W}} \rangle = \Psi_{\mathcal{W}}(\sigma^z) e^{J_{lm}^z \delta_\tau} \cosh(2J_{lm}^{xy} \delta_\tau)$$

$$- \Psi_{\mathcal{W}}(\sigma_1^z, \cdots - \sigma_l^z, \cdots - \sigma_m^z \ldots) e^{J_{lm}^z \delta_\tau} \sinh(2J_{lm}^{xy} \delta_\tau) \qquad (168)$$

$$= C' \langle \sigma^z | \Psi_{\bar{\mathcal{W}}} \rangle, \qquad (169)$$

which is equivalent to

$$\sum_{\{h,d\}} \Psi_{\mathcal{W}} \left[1 - \tanh(2J_{lm}^{xy} \delta_\tau) e^{-2\sum_{n=l,m}(\sigma_n^z \sum_j h_j W_{nj} + a_n \sigma_n^z)} \right] = C \Psi_{\bar{\mathcal{W}}} \qquad (170)$$

and $C = (e^{-J_{lm}^z \delta_\tau} / \cosh(2J_{lm}^{xy} \delta_\tau)) C'$. Notice that, here, we keep the bias term a_n in Eq. (63) instead of applying the gauge transformation in Eq. (103).

For $\sigma_l^z \sigma_m^z = 1$, we obtain

$$\sum_{\{h,d\}} \Psi_{\mathcal{W}} e^{-2J_{lm}^z \delta_\tau} / \cosh(2J_{lm}^{xy} \delta_\tau) = C \Psi_{\bar{\mathcal{W}}}. \qquad (171)$$

To make these imaginary time evolutions exact, W_{nj} $(n = l, m)$ is updated to $\bar{W}_{nj}$ with the increment ΔW_{nj} as $\bar{W}_{nj} = W_{nj} + \Delta W_{nj}$ with

$$\Delta W_{lj} = -\Delta W_{mj} = -\frac{1}{2}(W_{lj} - W_{mj}). \qquad (172)$$

The new couplings $W'_{j[l]}$, Z_{lmj} and $W''_{n[l]}$ are also given by

$$W'_{j[l]} = -Z_{lmj} = -\frac{1}{2}(W_{lj} - W_{mj}) \qquad (173)$$

and from

$$2(W''_{l[l]} - W''_{m[l]}) = \log[-e^{-2a_{l-m}} \tanh(2J_{lm}^{xy} \delta_\tau)] \qquad (174)$$

and

$$2\cosh(W''_{l[l]} + W''_{m[l]}) = \frac{e^{-2J_{lm}^z \delta_\tau - W''_{l-m}}}{\cosh(2J_{lm}^{xy} \delta_\tau)}, \qquad (175)$$

we obtain

$$W''_{l[l]} = \frac{1}{4}\left[\log\left[-e^{-2a_{l-m}} \tanh(2J_{lm}^{xy} \delta_\tau)\right] + 2\text{arcosh}\left[\frac{e^{-2J_{lm}^z \delta_\tau}}{\sqrt{-2e^{-2a_{l-m}} \sinh(4J_{lm}^{xy} \delta_\tau)}}\right]\right] \qquad (176)$$

$$W''_{m[l]} = \frac{1}{4}\left[-\log\left[-e^{-2a_{l-m}} \tanh(2J_{lm}^{xy} \delta_\tau)\right] + 2\text{arcosh}\left[\frac{e^{-2J_{lm}^z \delta_\tau}}{\sqrt{-2e^{-2a_{l-m}} \sinh(4J_{lm}^{xy} \delta_\tau)}}\right]\right] \qquad (177)$$

with $a_{l-m} = a_l - a_m$. On a bipartite lattice, to avoid the negative sign (or complex phase) problem we need to keep $W''_{l[l]}$ and $W''_{m[l]}$ real.

This can be achieved by choosing $a_l = 0$ for any l if $J_{lm} < 0$ (ferromagnetic case). For $J_{lm} > 0$ (antiferromagnetic case), $a_l = n\pi i$ with an arbitrary integer n if the site l belongs to the sublattice A and $a_l = (n + 1/2)\pi i$ if l belongs to the sublattice B. This local gauge for $J_{lm} > 0$ is equivalent to take $J_{lm}^{xy} \to -J_{lm}^{xy}$ and $a_l = 0$ for any site l as is

formulated in Eq.(103). We further note that $W''_{m[l]}$ can be taken positive if we take sufficiently small δ_τ in Eq. (177), with the leading order term $-\log(2J^{xy}_{lm}\delta_\tau)/2$. On the other hand, in Eq. (176), the leading order term is negative ($= -J_{lm}\delta_\tau$).

Recovery of the standard DBM form. To recover the original form of the DBM, we first use Eq. (69) with the replacement $s_1 \to \sigma^z_n$, $s_2 \to d_{[l]}$, $s_3 \to h_{[n]}$, $C \to D_n$, $V \to W''_{n[l]}$, $\tilde{V}_1 \to W_{n[n]}$ and $\tilde{V}_2 \to W'_{[n][l]}$ for $n = l, m$. We have added here two hidden variables $h_{[l]}$ and $h_{[m]}$. Then a solution for D_n, $W_{n[n]}$, and $W'_{[n][l]}$ are represented by using $W''_{n[l]}$ as

$$D_n = \frac{1}{2}\exp[-W''_{n[l]}] \tag{178}$$

$$W_{n[n]} = W'_{[n][l]} = \frac{1}{2}\mathrm{arcosh}(\exp[2W''_{n[l]}]), \tag{179}$$

if $W''_{n[l]}$ is positive (as in the case of $W''_{m[l]}$ for small δ_τ), which gives real $W_{n[n]}$ and $W'_{[n][l]}$. On the other hand, if $W''_{n[l]}$ is negative (as in the case of $W''_{l[l]}$ for small δ_τ), we should take

$$D_n = \frac{1}{2}\exp[W''_{n[l]}] \tag{180}$$

$$W_{n[n]} = -W'_{[n][l]} = \frac{1}{2}\mathrm{arcosh}(\exp[-2W''_{n[l]}]), \tag{181}$$

to give real $W_{n[n]}$ and $W_{[n][l]}$.

To completely recover the original DBM form, we next use Eq. (74) by replacing σ_1 with σ^z_l, σ_2 with σ^z_m, d_1 with $d_{[l]}$, d_2 with $d_{[lm]}$, h_1 with h_j, h_2 with $h_{[lm1]}$, h_3 with $h_{[lm2]}$, and V with Z_{lmj}.

With these solutions, by ignoring the trivial constant factors including D_l and D_m, the evolution is described by introducing two deep and four hidden additional variables $d_{[l]}$, $d_{[lm]}$, $h_{[l]}$, $h_{[m]}$, $h_{[lm1]}$, and $h_{[lm2]}$ as

$$
\begin{aligned}
\Psi_{\bar{\mathcal{W}}}(\sigma^z) = \sum_{\{\bar{h},\bar{d}\}} P_1(\sigma^z, h) P_2(h, d) \exp\Big[& \sum_{j,n=l,m} \sigma^z_n h_j \Delta W_{nj} + \sum_j h_j d_{[l]} W'_{j[l]} \\
& + \sum_{n=l,m} h_{[n]}(\sigma^z_n W_{n[n]} + d_{[l]}W'_{[n][l]}) + d_{[lm]}\sum_j h_j Z_{lmj} \\
& + \frac{i\pi}{4}(h_{[lm1]} + h_{[lm2]})(\sigma^z_l + \sigma^z_m + d_{[l]} + d_{[lm]})\Big],
\end{aligned}
\tag{182}
$$

where $\{\bar{h}, \bar{d}\}$ is a set consisting of the existing and new neurons. Equation (182) recovers the standard form of deep Boltzmann machine, where the physical spins σ^z as well as the deep variables d are not interacting each other and couples only to the hidden variables h.

Summary. After summing over $\{\bar{h}\}$, we reach

$$
\begin{aligned}
\Psi_{\bar{\mathcal{W}}}(\sigma) = \sum_{\{\bar{d}\}} \exp[\sum_{n=l,m} a_n \sigma^z_n] \prod_j \Big[2\cosh[\sum_i \sigma^z_i W_{ij} + \sum_k W'_{jk}d_k + d_{[l]}W'_{j[l]} + d_{[lm]}Z_{lmj}]\Big] \\
\times \prod_{n=l,m}\Big(2\cosh[\sigma^z_n W_{n[n]} + d_{[l]}W'_{[n][l]}]\Big)\Big[2\cos[\frac{\pi}{4}(\sigma^z_l + \sigma^z_m + d_{[lm]} + d_{[lm]})]\Big]^2
\end{aligned}
\tag{183}
$$

where the parameters W, W' and Z are given in Eqs. (172), (173), (176), (177), and (179) (or (181)).

We have introduced 2 deep and 4 hidden variables. Among them, $h_{[lm1]}$ and $h_{[lm2]}$ are simply to relate $d_{[l]}$ and $d_{[lm]}$ to σ^z_l and σ^z_m. With this trick, one can constrain $d_{[l]} = d_{[lm]}$ for $\sigma^z_l = \sigma^z_m$ and $d_{[l]} = -d_{[lm]}$ for $\sigma^z_l = -\sigma^z_m$. After repeatedly operating Eq. (182), for all the combinations of l, m, the DBM structure becomes nonlocal as we see in Fig. 7. After the sufficiently long imaginary-time evolution, with the analytical sum on $\{h\}$ and the Monte sampling over $\{d\}$, one can obtain the ground state wave function.
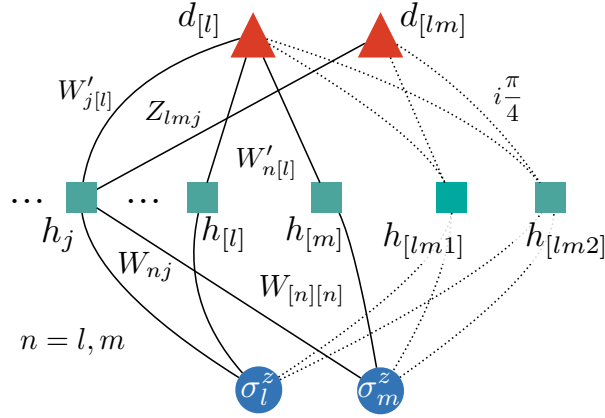
Figure 7. **Schematic picture for 2d-4h DBM network**. Dots, squares, triangles represent physical (σ_i^z), hidden (h_j), deep (d_k) variables. In 2d-4h construction, both W and W' couplings become nonlocal.

III. SAMPLING

Once we have determined specific rules to obtain the parameters of the DBM, the remaining question to be addressed is how to compute expectation values of physical quantities. Consider a quantum operator $\mathcal{O}$, then its expectation value over the DBM is given by the expression

$$\langle \mathcal{O} \rangle = \frac{\sum_{\{\sigma^z, h, h'd, d'\}} \Pi(\sigma^z, h, h', d, d') O_{\text{loc}}(\sigma^z, h, h')}{\sum_{\{\sigma^z, h, h'd, d'\}} \Pi(\sigma^z, h, h', d, d')}, \tag{184}$$

where we have introduced the pseudo-probability density $\Pi(\sigma^z, h, h', d, d') \equiv P_1(\sigma^z, h) P_2(h, d) P_1^\star(\sigma^z, h') P_2^\star(h', d')$, and the "local" estimator $O_{\text{loc}}(\sigma^z, h, h') = \frac{1}{2} \sum_{\{\sigma'^z\}} \langle \sigma^z | \mathcal{O} | \sigma'^z \rangle \left(\frac{P_1(\sigma'^z, h)}{P_1(\sigma^z, h)} + \frac{P_1(\sigma'^z, h')^\star}{P_1(\sigma^z, h')^\star} \right)$. For a large number of spins and hidden/deep units, it is not possible to compute those sums numerically, because of the exponential number of terms involved. However, there are specific cases in which efficient sampling strategies can be devised, allowing to stochastically compute the quantum expectation values. In general, when the DBM weights are all real $\Pi(\sigma^z, h, h', d, d') \geq 0$, and it can be interpreted as an (unnormalized) probability density. Thus, Markov-chain sampling techniques can be applied, similarly to the case of applications in standard machine learning. In the case of complex-valued weights, the straightforward probabilistic interpretation breaks down, and a sign (phase) problem arises. However, there are specific cases in which one can still recover a properly defined probability density, and efficiently sample from it. In the following we describe two main sampling methods based on Markov chain techniques. First, Gibbs sampling, then Metropolis-Hastings sampling. In both cases we discuss when the sign problem can be circumvented.

A. Gibbs sampling

We start discussing a strategy which is the natural generalization of what traditionally used in most applications of DBM in machine learning. The approach is based on Gibbs sampling, a strategy which amounts to generate samples using the exact conditional probabilities for block of variables. In practice, we introduce three kind of moves, which allow to generate a Markov chain of visible, hidden, and deep variables distributed according to $\Pi(\sigma^z, h, h', d, d')$.

1. Sampling visible spins

The first kind of move consists in freezing all the hidden and deep variables, and sampling the visible spins σ^z. Specifically, we generate new visible spin configurations according to the conditional probability:

$$\Pi(\sigma^z|h,h',d,d') = \frac{P_1(\sigma^z,h)P_2(h,d)P_1^\star(\sigma^z,h')P_2^\star(h',d')}{\sum_{\{\tilde{\sigma}^z\}} P_1(\tilde{\sigma}^z,h)P_2(h,d)P_1^\star(\tilde{\sigma}^z,h')P_2^\star(h',d')}$$

$$= \frac{P_1(\sigma^z,h)P_1^\star(\sigma^z,h')}{\sum_{\{\tilde{\sigma}^z\}} P_1(\tilde{\sigma}^z,h)P_1^\star(\tilde{\sigma}^z,h')}$$

$$= \frac{\Pi_i^N \exp\left\{\sigma_i^z \left[\sum_j \left(h_j W_{ij} + h_j' W_{ij}^\star\right) + 2a_i^{\mathrm{r}}\right]\right\}}{\Pi_i^N 2\cosh\left(\sum_j \left(h_j W_{ij} + h_j' W_{ij}^\star\right) + 2a_i^{\mathrm{r}}\right)}.$$

Here, a_i^{r} is a real part of a_i. A particularly appealing aspect of this transition probability is that each visible spin can be treated independently from the others, thus we can update in parallel all visible spins at once. The probability of a given spin to be up for example is:

$$P(\sigma_i^z = 1|h,h',d,d') = \text{Logistic}(2\lambda_i^{[\sigma^z]}), \tag{185}$$

with $\lambda_i^{[\sigma^z]} = \sum_j \left(h_j W_{ij} + h_j' W_{ij}^\star\right) + 2a_i^{\mathrm{r}}$, and $\text{Logistic}(x) = \frac{1}{1+\exp(-x)}$. Thus, during this phase we generate N random numbers η_i uniformly distributed in $[0,1)$, and set the spin $\sigma_i^z = 1$ if $\eta_i < \text{Logistic}(2\lambda_i^{[\sigma^z]})$. For this approach to be feasible, we must have that the $\lambda_i^{[\sigma^z]}$ are real. Necessary conditions for this condition to be satisfied are discussed at the end of this section.

2. Sampling hidden spins

The second type of move consists in freezing visible and deep spins, and sampling hidden variables h and h'. For example, to sample h the transition probability reads:

$$\Pi(h|\sigma^z,h',d,d') = \frac{P_1(\sigma^z,h)P_2(h,d)}{\sum_{\{\tilde{h}\}} P_1(\sigma^z,\tilde{h})P_2(\tilde{h},d)}$$

$$= \frac{\Pi_j^M \exp\left[h_j \left(\sum_i \sigma_i^z W_{ij} + b_j + \sum_k d_k W_{jk}'\right)\right]}{\Pi_j^M 2\cosh\left(\sum_i \sigma_i^z W_{ij} + b_j + \sum_k d_k W_{jk}'\right)}.$$

The probability of having $h_j = 1$ is then:

$$P(h_j = 1|\sigma^z,h',d,d') = \text{Logistic}(2\lambda_j^{[h]}), \tag{186}$$

with $\lambda_j^{[h]} = \sum_i \sigma_i^z W_{ij} + b_j + \sum_k d_k W_{jk}'$. Again, one can therefore efficiently update all the M hidden spins at once, without rejection. Analogously, for h' we have $\lambda_j^{[h']} = \sum_i \sigma_i^z W_{ij}^\star + b_j^\star + \sum_k d_k' W_{jk}'^\star$.

3. Sampling deep spins

The final set of moves consists in freezing visible and hidden spins, and sample from deep variables d and d'. For example, to sample d the transition probability is:

$$\Pi(d|\sigma^z,h,h',d') = \frac{P_2(h,d)}{\sum_{\{\tilde{d}\}} P_2(h,\tilde{d})}$$

$$= \frac{\Pi_k^{M'} \exp\left[d_k \left(\sum_j h_j W_{jk}' + c_k\right)\right]}{\Pi_k^{M'} 2\cosh\left(\sum_j h_j W_{jk}' + c_k\right)}.$$

The probability of having $d_k = 1$ is then:

$$P(d_k = 1|\sigma^z, h, h', d') = \text{Logistic}(2\lambda_k^{[d]}),$$ (187)

with $\lambda_k^{[d]} = \sum_j h_j W'_{jk} + c_k$. Analogously, we have $\lambda_k^{[d']} = \sum_j h'_j W'^{\star}_{jk} + c_k^{\star}$.

4. Overall scheme: alternate block sampling

The overall sampling scheme is therefore realized putting together all those individual Gibbs samplings. In particular, we can devise a two-step block sampling, which takes into account the conditional dependence of all the probabilities previously derived.

The overall sampling scheme then works as follow:

1. Sample h and h', fixing all the other variables. This is realized using the probabilities (186) for all the hidden spins.

2. Sample σ^z,d,d' fixing the values of h and h'.This is realized using the probabilities (87) and (187) for all the visible and deep spins, respectively.

3. Cycle between 1 and 2.

5. Phase problem in the Gibbs scheme

In order to get a consistent sampling scheme, we must have that all the quantities $\lambda_i^{[\sigma^z]}, \lambda_j^{[h]}, \lambda_j^{[h']}, \lambda_k^{[d]}, \lambda_k^{[d']}$ are real valued. In the absence of this condition, we have a phase problem, and we cannot directly use a stochastic approach to sample from the DBM. Looking more closely at what conditions are needed, we start noticing that the visible bias can take arbitrary (complex) values, since only the real parts, a_i^{r}, enter $\lambda_i^{[\sigma^z]}$. In general, there might be specific choices of the DBM parameters which still guarantee absence of phase problem. One possibility is realized, for example, when fixing the total magnetizations in the three layers, i.e. the constraints $\sum_i \sigma_i^z = \sigma_{\text{tot}}^z$, $\sum_j h_j = h_{\text{tot}}$, $\sum_k d_k = d_{\text{tot}}$. We further assume that $\text{Im}(W_{ij}) = W^{\text{I}}$, a constant, as well as $\text{Im}(W'_{jk}) = W'^{\text{I}}$. Then, it is easy to see that the phase problem is avoided when $b_j^{\text{I}} = -\sigma_{\text{tot}}^z W^{\text{I}} - d_{\text{tot}} W'^{\text{I}}$ and $c_k^{\text{I}} = -h_{\text{tot}} W'^{\text{I}}$. Notice that those are just a specific set of conditions, and less stringent ones can be found using other sampling schemes.

When each sample has the imaginary part or negative signs, another possibility of avoiding the phase problem is to take the partial trace summation explicitly so that such partial sum gives always a real nonnegative value. We will discuss this point in more detail in the next section.

B. Metropolis sampling

1. Marginal probability density

Because there are no intralayer interactions in the DBM architecture, one can analytically trace out either one of h, h' and d, d'. Then we get marginal probability density: $\tilde{\Pi}(\sigma^z, h, h') = \sum_{\{d,d'\}} \Pi(\sigma^z, h, h', d, d')$ or $\tilde{\Pi}'(\sigma^z, d, d') = \sum_{\{h,h'\}} \Pi(\sigma^z, h, h', d, d')$. Defining $\tilde{P}(\sigma^z, h)$ and $\tilde{P}'(\sigma^z, d)$ as

$$\tilde{P}(\sigma^z, h) = \sum_{\{d\}} P_1(\sigma^z, h) P_2(h, d) = e^{\sum_i a_i \sigma_i^z + \sum_{ij} \sigma_i^z h_j W_{ij} + \sum_j b_j h_j} \times \prod_k 2\cosh\left(c_k + \sum_k h_j W'_{jk}\right)$$ (188)

and

$$\tilde{P}'(\sigma^z, d) = \sum_{\{h\}} P_1(\sigma^z, h) P_2(h, d) = \prod_j 2\cosh\left(b_j + \sum_i \sigma_i^z W_{ij} + \sum_k d_k W'_{jk}\right) \times e^{\sum_i a_i \sigma_i^z + \sum_k c_k d_k},$$ (189)

respectively, the marginal probability densities are given by

$$\tilde{\Pi}(\sigma^z, h, h') = \sum_{\{d,d'\}} \Pi(\sigma^z, h, h', d, d') = \tilde{P}(\sigma^z, h)\tilde{P}^\star(\sigma^z, h'), \tag{190}$$

$$\tilde{\Pi}'(\sigma^z, d, d') = \sum_{\{h,h'\}} \Pi(\sigma^z, h, h', d, d') = \tilde{P}'(\sigma^z, d)\tilde{P}'^\star(\sigma^z, d'). \tag{191}$$

With these marginal probability densities, we perform the Metropolis sampling to measure physical quantities. The expectation value of a quantum operator $\mathcal{O}$ is given by

$$\langle \mathcal{O} \rangle = \frac{\sum_{\{\sigma^z, h, h'\}} \tilde{\Pi}(\sigma^z, h, h')\tilde{O}_{\text{loc}}(\sigma^z, h, h')}{\sum_{\{\sigma^z, h, h'\}} \tilde{\Pi}(\sigma^z, h, h')} = \frac{\sum_{\{\sigma^z, d, d'\}} \tilde{\Pi}'(\sigma^z, d, d')\tilde{O}'_{\text{loc}}(\sigma^z, d, d')}{\sum_{\{\sigma^z, d, d'\}} \tilde{\Pi}'(\sigma^z, d, d')} \tag{192}$$

with

$$\tilde{O}_{\text{loc}}(\sigma^z, h, h') = \frac{1}{2} \sum_{\{\sigma'^z\}} \langle \sigma^z | \mathcal{O} | \sigma'^z \rangle \left(\frac{\tilde{P}(\sigma'^z, h)}{\tilde{P}(\sigma^z, h)} + \frac{\tilde{P}(\sigma'^z, h')^\star}{\tilde{P}(\sigma^z, h')^\star} \right), \tag{193}$$

$$\tilde{O}'_{\text{loc}}(\sigma^z, d, d') = \frac{1}{2} \sum_{\{\sigma'^z\}} \langle \sigma^z | \mathcal{O} | \sigma'^z \rangle \left(\frac{\tilde{P}'(\sigma'^z, d)}{\tilde{P}'(\sigma^z, d)} + \frac{\tilde{P}'(\sigma'^z, d')^\star}{\tilde{P}'(\sigma^z, d')^\star} \right). \tag{194}$$

2. Phase problem in the Metropolis scheme

An advantage of choosing the marginal probability density is that by taking the summation over h and d, the sign problem can sometimes be avoided even if the DBM has complex parameters. An example is to take the summation over the hidden variables h analytically in the three DBM constructions for the Heisenberg models presented in Sec. II B. In all the three cases, only those W and W' couplings used to enforce the constraints are complex-valued, and the summation over h eliminates the negative weight. For example, in the case of the 2d-4h representation in Sec. II B 3, though each sample may have a finite imaginary part as in each term of Eq. (182), the total weight becomes real and nonnegative, after the explicit summation over the h degrees of freedom is performed as in Eq. (183).

When the lattice is not bipartite, we can still write down the DBM solutions to exactly follow the imaginary time evolutions. However, in this case, we will have imaginary W and W' parameters even for the units not involved in enforcing the constraints. In this case, the sampling may suffer from sign problem. However, as we discuss in the main text, in contrast to the conventional quantum Monte Carlo simulations, we can make the number of imaginary time step to reach the ground state short by starting the analytical DBM time evolution [Eq. (78)] from a good stating point $|\Psi_0\rangle$. For example, numerically optimized RBM wave functions can be used for $|\Psi_0\rangle$, or more generally, $|\Psi_0\rangle$ can be wave functions used in the conventional wave function techniques. In this case, before we suffer from a severe sign problems, we might be able to reach the ground state with good statistical accuracy.

3. Overall scheme

We sample over σ^z, h, h' [or σ^z, d, d'] with the marginal probability density $\tilde{\Pi}(\sigma^z, h, h')$ [$\tilde{\Pi}'(\sigma^z, d, d')$]. The physical quantities are measured following Eq. (192). In the case of Heisenberg model, after tracing out the h spins, we have constraints over the values of σ^z, d, d'. In that case, a cluster update rather than a local update will be more efficient. In particular, in the 2d-6h representation, since the imaginary-time evolution of the DBM is equivalent to the path-integral formalism, we can apply an efficient cluster update used in the conventional quantum Monte Carlo method, such as so called loop update [40].